P values are based on 2-sided tests of significance and values of <0.05 were considered significant for all analyses.

## RESULTS

### MtDNA Levels in Treatment Naive HIV-1-Infected Patients and Healthy Controls

As shown in Figure 1, mtDNA levels were significantly lower in treatment-naive HIV-1-infected patients (n = 46) than in healthy controls (0.430 ± 0.190 vs 0.617 ± 0.307, $P = 0.0006$). Interestingly, mtDNA levels in HIV-1-infected patients demonstrated a significantly positive correlation with $CD4^+$ T-cell count (n = 45. rs = 0.333, $P = 0.028$) and an inverse correlation with HIV RNA copies (n = 33, rs = −0.423, $P = 0.017$) (Fig. 2). The patients who were untreated throughout the study period (Fig. 1C; n = 13) exhibited low viral loads and high $CD4^+$ T-cell counts, and the majority of them appeared to be candidates of long-term non-progressors. These subjects had significantly higher $CD4^+$ T-cell counts and lower HIV-1 RNA copies at baseline than patients for whom treatment was initiated (n = 33) (Table I). The treated subjects (Fig. 1B) had significantly lower mtDNA levels than healthy people (Fig. 1D) (0.399 ± 0.143 vs 0.617 ± 0.307, $P = 0.0002$), while the untreated subjects (Fig. 1C) showed no significant difference in mtDNA levels (0.508 ± 0.268 vs 0.617 ± 0.307, $P = 0.178$). There were no significant correlations observed between mtDNA and other clinical parameters except GOT (n = 39, rs = −0.348, $P = 0.030$) and TG (n = 31, rs = −0.512, $P = 0.005$) (data not shown).

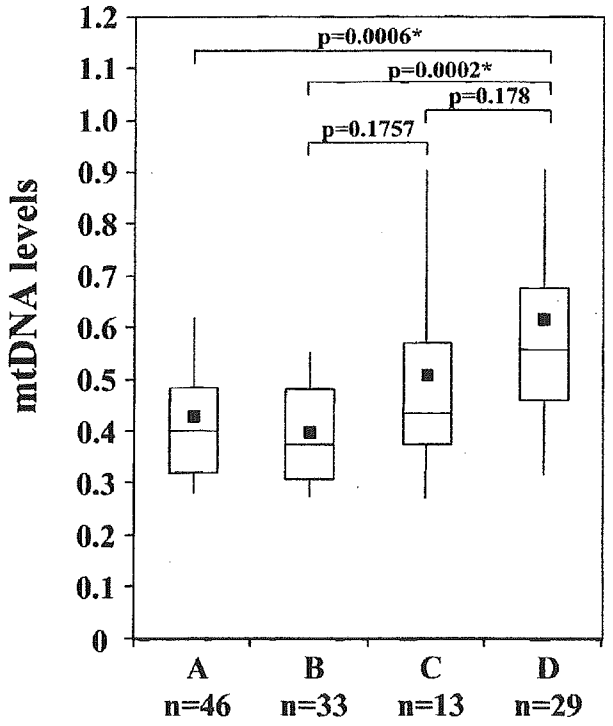


Fig. 1. Comparison of mtDNA levels between treatment-naive HIV-1-infected patients and healthy controls. Comparative box plots of mtDNA in treatment-naive HIV-1-infected patients and healthy controls. The upper and lower ends of the vertical lines indicate the 90th and 10th percentiles, respectively. The top and bottom of the box indicate the 75th and 25th percentiles, respectively. The middle lines and solid squares indicate median and mean, respectively. A: all patients involved this study, B: patients treated thereafter, C: patients remain untreated, D: healthy controls. Data were analyzed by Mann-Whitney U-test. * indicates statistical significance.

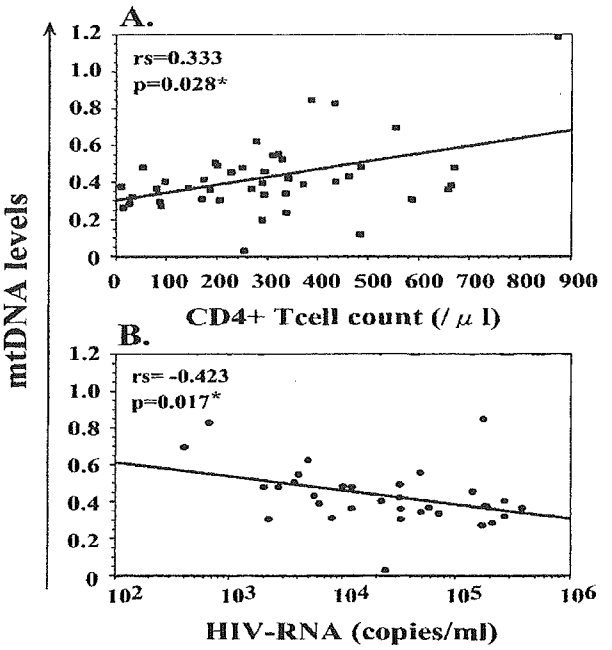


Fig. 2. Correlation between $CD4^+$ T-cell count (**A**) or HIV-1 RNA copies (**B**) and mtDNA amount in treatment-naive HIV-1-infected patients. $CD4^+$ T-cell count had been measured in only 45 of 46 subjects and HIV viral load in only 33 of 46 subjects. Solid lines indicate the results of simple regression analysis. Data were analyzed by Spearman's ranks test. * indicates statistical significance.

### Longitudinal mtDNA Quantification

In longitudinal quantification, mtDNA levels of untreated HIV-1-infected patients and healthy controls (only 11of 29 healthy controls were analyzed at multiple time points) were stable through out our observation period (Fig. 3B,C). $CD4^+$ T-cell counts of untreated patients in this cohort were also stable and were not significantly different between baseline levels and after 500–1,000 (797 ± 104) days [n = 11 (only 11 of 13 had available baseline data), 535.5 ± 155.4 vs 512.0 ± 181.9/μl, $P = 0.721$, paired $t$-test].

When we analyzed mtDNA levels in all treated patients together, we found a significant increase in mtDNA levels after about 1,000 days of treatment (Fig. 3A). There was a tendency towards an increase in levels among healthy controls, though this difference was not statistically significant (1,000–1,500 days vs healthy, 0.888 ± 0.753 vs 0.617 ± 0.307, $P = 0.0549$, Mann-Whitney U-test).We then selected 25 patients as described in the previous section. MtDNA levels in the

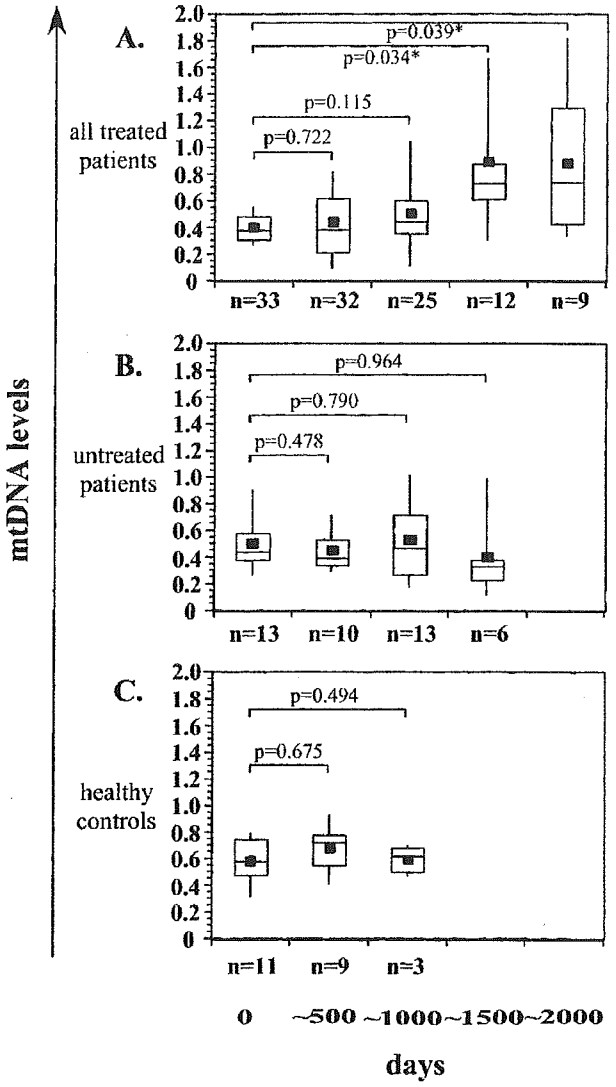


Fig. 3. Time course of mtDNA levels in HIV-1-infected patients and healthy controls. **A–C**: Time course of all patients treated by any antiretroviral regimens, untreated patients and healthy controls, respectively. The vertical axis and the markers of box plot are the same as in Fig. 1. Horizontal axis shows observed periods divided every 500 days. We chose only one data point from a person in one period. If there was more than one data point available from a person in one period, the data nearest to the median in the period was chosen. Since the follow-up periods were different among individuals, the number of persons used for analysis of each period was shown below the horizontal axis. Data were analyzed by the paired *t*-test. * indicates statistical significance.

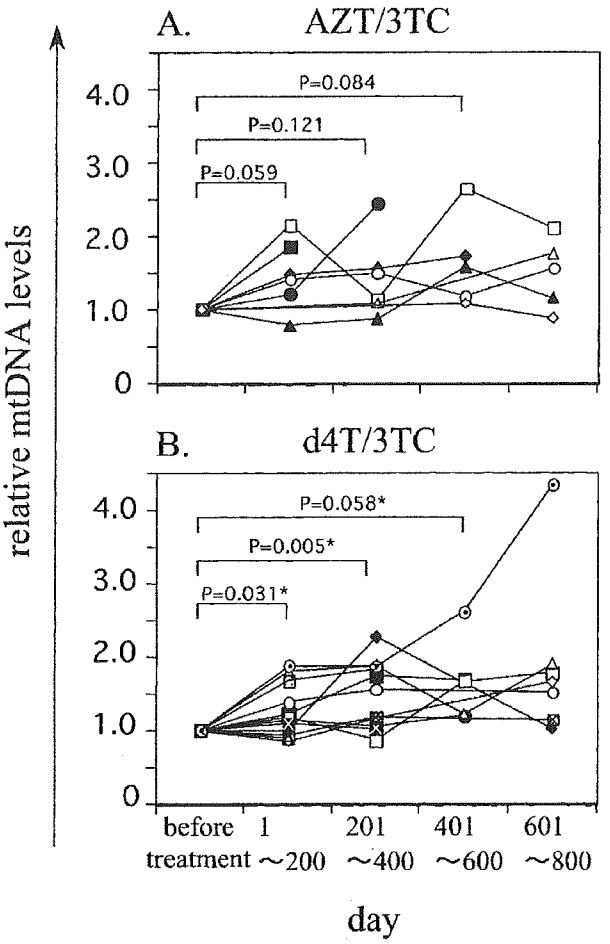


Fig. 4. Individual changes of mtDNA levels in HIV-1-infected patients treated with regimens containing AZT/3TC or d4T/3TC. Vertical axis indicates relative mtDNA levels from baseline. Horizontal axis indicate duration of therapy segmented every 200 days. **A** and **B** show the results of AZT/3TC and d4T/3TC, respectively. All presented data are the mean value of triplicate experiments. Average standard deviations were $13.7 \pm 6.9$ and $13.2 \pm 6.0\%$ of mean values, respectively. Data were analyzed by the paired *t*-test. * indicates statistical significance.

patients treated with AZT/3TC (n = 8) or d4T/3TC (n = 12) containing regimens increased shortly after the initiation of treatments, although only the d4T/3TC group demonstrated a statistically significant difference (Fig. 4). However, since the trends of both groups were similar, we grouped them together for further analysis. As shown in Figure 5A, the AZT(or d4T)/3TC-treated group showed a significant increase in mtDNA levels during treatment. In about 400–600 days, mtDNA levels recovered to levels comparable to healthy controls ($0.547 \pm 0.161$ vs $0.617 \pm 0.307$, $P = 0.748$, Mann Whitney U-test). By contrast, the AZT/ddC-treated group demonstrated a significant decrease in mtDNA levels within 200 days and remained at low levels for more than 500 days (Fig. 5B). These observations were confirmed by amplification of Mt2 (Fig. 5C,D).

### Detailed Analysis of AZT/ddC Group

As we have shown above, mtDNA levels in treatment-naive HIV-1-infected patients is correlated with $CD4^+$ T-cell count. We therefore set out to further characterized the relationship in the AZT/ddC-treated group. $CD4^+$ T-cell counts increased after initiation of antiretroviral therapy in 3 patients, while mtDNA levels decreased in all 5 (Fig. 6). In one patient for whom we instituted a short treatment interruption due to

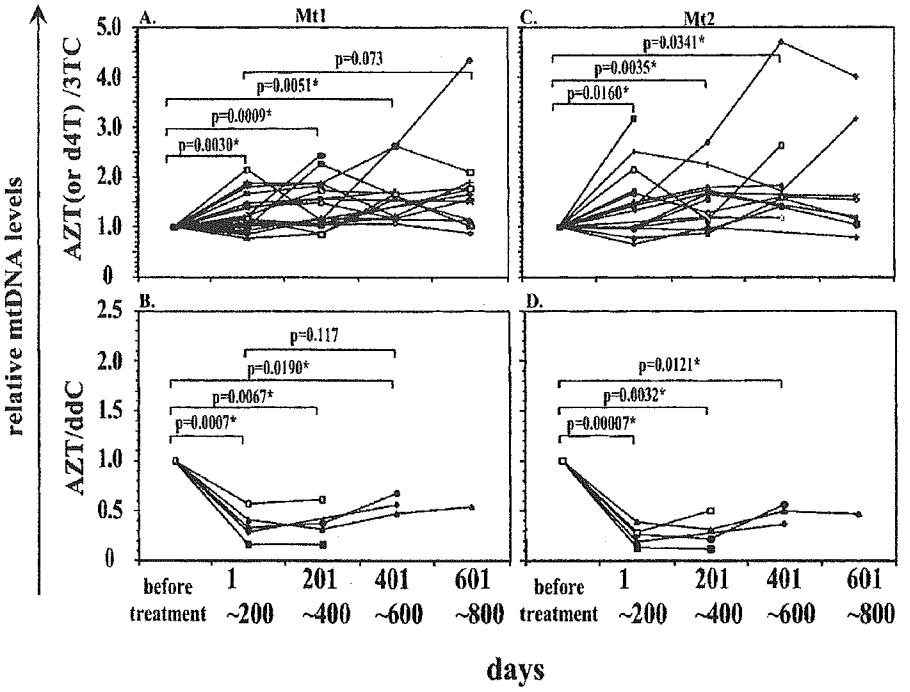


Fig. 5. Individual changes of mtDNA levels in HIV-1-infected patients grouped according to backbone nucleosides, The left two panels (**A** and **B**) show the results of Mt1 amplification. The right two (**C** and **D**) show Mt2 as well. Mt2 were measured in some of patients. A and C are the results of AZT(or d4T)/3TC groups, B and D show the results of AZT/ddC group. All presented data are the mean value of triplicate experiments. Average standard deviations were $13.5 \pm 6.5$ and $14.3 \pm 7.6\%$ of mean values, respectively. The identical symbols in Mt1 and Mt2 indicate the same patients. Data were analyzed by the paired $t$-test. * indicates statistical significance.

infection with hepatitis A (indicated by a triangle in the corresponding figure), mtDNA levels decreased rapidly within one month after initiation of AZT/ddC/NFV and recovered quickly when the treatment was interrupted. After treatment was resumed, mtDNA levels decreased again.

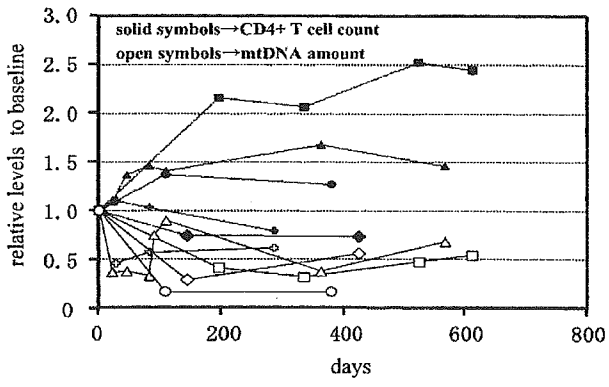


Fig. 6. Relationship between mtDNA levels and $CD4^+$ T-cell count in the patients treated with regimens containing AZT/ddC. Vertical axis shows relative amount from baseline. Open symbols indicate mtDNA amount measured as Mt1 and solid ones indicate $CD4^+$ T-cell count. Symbols with identical shapes represent data from the same patient. The patient indicated as a triangle had a treatment interruption within 1 month. mtDNA in this patient increased rapidly and returned to baseline levels.

## Comparison of Clinical Parameters Between AZT/ddC and AZT (or d4T)/3TC Groups

Since there was a considerable difference in mtDNA levels between the AZT/ddC-treated group and the AZT(or d4T)/3TC-treated group, we compared changes in blood cell counts and biochemistries 360 days after treatment. There were significant differences in $CD4^+$ T-cell ($1.308 \pm 0.513$ vs $4.062 \pm 4.039$-fold from baseline, $P = 0.031$, Mann-Whitney U-test), $CD8^+$ T-cell ($0.632 \pm 0.282$ vs $1.554 \pm 0.707$-fold from baseline, $P = 0.0132$, Student's $t$-test) and HIV RNA copies ($0.227 \pm 0.310$ vs $0.028 \pm 0.046$-fold from baseline, $P = 0.038$, Mann-Whitney U-test), but not in other parameters (data not shown).

## Correlation Between mtDNA and Blood Lactate Levels

We found no significant correlation between mtDNA and blood lactate levels in 13 asymptomatic patients on antiretroviral therapy (0.59~2.91 mmol/l, $r = 0.442$, $P = 0.131$, Pearson's correlation coefficients test).

## MtDNA Levels in Patients with Lipoatrophy or Peripheral Neuropathy

According to the previously given definition, 20 of 33 (60.6%) patients were lipoatrophic. We compared the

change in mtDNA levels from baseline between patients with and without lipoatrophy. For this analysis, we used the DNA samples drawn closest to the day when the diagnosis of lipoatrophy was made (mean ±1 SD; 986.7 ± 567.2 days). However, we did not observe a statistically significant difference(with vs without: 3.43 ± 5.04 vs 1.95 ± 1.02-fold from baseline, $P = 0.606$, Mann-Whitney U-test). Four patients developed relatively severe peripheral neuropathy, clinically diagnosed by a neurologist; however, we did not find mtDNA depletion while their symptoms existed (data not shown).

## DISCUSSION

Our finding that treatment-naive HIV-1-infected patients demonstrate mtDNA depletion in PBMCs is concordant with a recent report by Cote et al. [2002]. We found further that mtDNA level was not only positively correlated with $CD4^+$ T-cell count, but also inversely correlated with plasma viral loads. Moreover, baseline mtDNA depletion was ameliorated at least by AZT/3TC or d4T/3TC containing regimens (in these groups, HIV-RNA had been well suppressed and $CD4^+$ T-cell count had remarkably increased after 360 days of treatment). Although we could not detect statistically significant differences in the AZT/3TC-treated group, the trends found in this group and the d4T/3TC-treated groups were similar, and the failure to find a statistical difference in the former group could be due to insufficient sample size. There was no significant difference in the change of $CD4^+$ T-cell counts after 360 days of treatment between them (1.43 ± 0.56 vs 1.50 ± 0.40-fold from baseline, $P = 0.758$, Student's $t$-test). As mentioned earlier, Cossarizza et al. reported that there was no difference in mtDNA content in peripheral blood lymphocytes among HIV-1-infected children with lipodystrophy, those without lipodystrophy and healthy controls [Cossarizza et al., 2002]. McComsey et al. reported that patients with lipoatrophy have higher mtDNA levels in peripheral blood leucocytes than treatment-naive patients, although the difference was not statistically significant [McComsey et al., 2002]. Their results may support ours that mtDNA in treatment-naive patients might recover after initiation of antiretroviral therapy.

Based on these results, it is tempting to speculate that HIV-1-infection itself may cause mtDNA depletion. Much evidence, both in vivo and in vitro, suggest that mitochondria-mediated apoptosis may play an important role in $CD4^+$ T-cell depletion in HIV-1 infection [Macho et al., 1995; Carbonari et al., 1997; Cossarizza et al., 1997; Macho et al., 1999; Ferri et al., 2000a,b; Jacotot et al., 2000; Moretti et al., 2000; Rasola et al., 2001; Roggero et al., 2001; Petit et al., 2002]. MtDNA depletion in PBMCs may be related to but would not explained by $CD4^+$ T-cell apoptosis per se. As we showed in Figure 2A, mtDNA level was correlated with $CD4^+$ T-cell count. The contribution of $CD4^+$ T cells to mtDNA levels in whole PBMCs should be small in patients with advanced disease who have very low $CD4^+$ T-cell counts. Therefore, additional cell types such as $CD8^+$ T cells should be involved. $CD8^+$ T-cell turnover is increased in HIV-1 infection [Hellerstein et al., 1999]; therefore, the mechanism for mtDNA depletion in PBMCs may be complicated.

McComsey et al. [2002] found that patients on antiretroviral therapy have significantly higher levels of mtDNA than healthy controls and speculated that this finding may be due to mitochondrial proliferation in response to unfavorable functioning in the presence of NRTIs. In the present study, we also observed that the treated patients as a whole had higher mtDNA levels than healthy controls at 1,000–1,500 days, although this difference was not significant. Therefore, the hypothesis proposed by McComsey and colleagues may help explain the increase in mtDNA levels observed in our study as well. Phenix et al. [2001] demonstrated that HIV protease inhibitors could inhibit mitochondria-mediated apoptosis. This mechanism might also contribute to the recovery of mtDNA to some extent.

The AZT/ddC-treated group showed a significant reduction in mtDNA levels after initiation of antiretroviral therapy. Since $CD4^+$ T-cell counts did recover in this group, although less than in the AZT (or d4T)/3TC-treated group, mtDNA depletion cannot be explained by $CD4^+$ T cells. The most probable explanation for this reduction would be the strong inhibitory effect of ddC on DNA polymerase $\gamma$ and mtDNA synthesis as demonstrated in vitro.

Recently, Cote et al. [2002] reported a further reduction in mtDNA levels of buffy coats in patients with symptomatic hyperlactatemia, most of whom were treated with regimens containing d4T/ddI. Since d4T and ddI exhibit a strong inhibitory effect on mtDNA synthesis next to ddC, this combination might cause additive or synergistic effects on mtDNA synthesis in vivo. Since we did not have patients treated with d4T/ddI in our study, we may have reached a different result.

Depleted MtDNA levels in patients with hyperlactatemia as reported by Cote et al. [2002] recovered after cessation of antiretroviral therapy. Similarly, in our study, mtDNA level of one patient in the AZT/ddC-treated group, who had experienced a short treatment interruption, did recover immediately after the interruption. It is likely that the inhibitory effect of antiretroviral therapies containing certain nucleoside analogues is reversible at least in the peripheral blood. It may be feasible to speculate that even in target organs consisting of non-dividing cells, mtDNA depletion might recover since mtDNA replication is semi-independent of chromosomal DNA.

MtDNA exists in a condition called "heteroplasmy" where wild-type and mutant mitochondrial genomes are mixed together. Moreover, it is thought that some NRTIs inhibit not only polymerase activity but also the 3′-5′exonuclease activity of DNA polymerase $\gamma$ [Lim and Copeland, 2001] and might cause mutations in mtDNA. To avoid a bias caused by a difference in the efficiency of the primers used to amplify mtDNA, we used two sets of

primers to validate our quantification. Since there is a common deletion of 5 kb in mtDNA which increases with aging [Berdanier and Everts, 2001], one of our primer sets was designed to amplify the DNA segment inside the common deletion (Mt1) and the other outside (Mt2). However, we did not observe obvious differences between them.

One of the initial aims of this study was to investigate the possibility of using quantification of mtDNA in PBMCs as an early predictor for adverse events occurring during antiretroviral therapy. Although the number of patients was small in this study, we found no significant difference in routine blood cell counts nor biochemistries between the AZT/ddC-treated group (mtDNA was decreased) and the AZT(or d4T)/3TC-treated group (mtDNA was increased). We also found no difference between lipoatrophic patients and non-lipoatrophic patients. There was no depletion of mtDNA during the course of peripheral neuropathy either. Although there were no patients with symptomatic lactatemia, we found no significant correlation between mtDNA and blood lactate levels. Taken together, quantification of mtDNA in PBMCs seems not to be a predictor of adverse effects caused by antiretroviral treatments. As described in the previous section, Cossariza et al. found no mtDNA depletion in children with lipodystrophy. Furthermore, McComsey et al. [2002] did not find depletion of mtDNA in patients with lipoatrophy, even in one patient with lactic acidosis. Their results are concordant with ours. On the contrary, Cote et al. [2002] reported mtDNA reduction in patients with symptomatic hyperlactatemia prior to lactate elevation. In their study, 7 of 8 patients were treated with a particular regimen containing d4T and ddI. While we quantified mtDNA in PBMCs, McComsey et al., Cossariza et al., and Cote et al. used peripheral blood leukocytes, lymphocytes and buffy coats, respectively. Up to now, no one has investigated difference in mtDNA levels in different subsets of peripheral blood cells. Since a direct role of HIV-1 on the metabolism of mtDNA was suggested and different antiretroviral regimens demonstrated different effects, larger studies are warranted to explore the mechanisms of mtDNA loss in HIV-1 infection as well as the role of mtDNA measurement in the care of HIV-1-infected patients.

## ACKNOWLEDGMENTS

The authors thank Hironobu Kikuchi and Yoichiro Mitsuishi (School of Medicine, University of Tohoku) for their excellent technical skills. We also thank Mr. David Chao for his comments on the language of manuscript, as well as Dr. Shuji Hashimoto (Department of Hygiene, Fujita Health University School of Medicine) for help with statistical analyses.

## REFERENCES

Arnaudo E, Dalakas M, Shanske S, Moraes CT, DiMauro S, Schon EA. 1991. Depletion of muscle mitochondrial DNA in AIDS patients with zidovudine-induced myopathy. Lancet 337:508–510.

Benbrik E, Chariot P, Bonavaud S, Ammi-Said M, Frisdal E, Rey C, Gherardi R, Barlovatz-Meimon G. 1997. Cellular and mitochondrial toxicity of zidovudine (AZT), didanosine (ddI) and zalcitabine (ddC) on cultured human muscle cells. J Neurol Sci 149:19–25.

Berdanier CD, Everts HB. 2001. Mitochondrial DNA in aging and degenerative disease. Mutat Res 475:169–183.

Brinkman K, Smeitink JA, Romijn JA, Reiss P. 1999. Mitochondrial toxicity induced by nucleoside-analogue reverse-transcriptase inhibitors is a key factor in the pathogenesis of antiretroviral-therapy-related lipodystrophy. Lancet 354:1112–1115.

Carbonari M, Pesce AM, Cibati M, Modica A, Dell'Anna L, D'Offizi G, Angelici A, Uccini S, Modesti A, Fiorilli M. 1997. Death of bystander cells by a novel pathway involving early mitochondrial damage in human immunodeficiency virus-related lymphadenopathy. Blood 90:209–216.

Carter VM, Hoy JF, Bailey M, Colman PG, Nyulasi I, Mijch AM. 2001. The prevalence of lipodystrophy in an ambulant HIV-infected population: it all depends on the definition. HIV Med 2:174–180.

Casademont J, Barrientos A, Grau JM, Pedrol E, Estivill X, Urbano-Marquez A, Nunes V. 1996. The effect of zidovudine on skeletal muscle mtDNA in HIV-1 infected patients with mild or no muscle dysfunction. Brain 119(Pt 4):1357–1364.

Cossarizza A, Mussini C, Mongiardo N, Borghi V, Sabbatini A, De Rienzo B, Franceschi C. 1997. Mitochondria alterations and dramatic tendency to undergo apoptosis in peripheral blood lymphocytes during acute HIV syndrome. AIDS 11:19–26.

Cossarizza A, Mussini C, Vigano A. 2001. Mitochondria in the pathogenesis of lipodystrophy induced by anti-HIV antiretroviral drugs: actors or bystanders? BioEssays 23:1070–1080.

Cossarizza A, Pinti M, Moretti L, Bricalli D, Bianchi R, Troiano L, Fernandez MG, Balli F, Brambilla P, Mussini C, Vigano A. 2002. Mitochondrial functionality and mitochondrial DNA content in lymphocytes of vertically infected human immunodeficiency virus-positive children with highly active antiretroviral therapy-related lipodystrophy. J Infect Dis 185:299–305.

Cote HC, Brumme ZL, Craib KJ, Alexander CS, Wynhoven B, Ting L, Wong H, Harris M, Harrigan PR, O'Shaughnessy MV, Montaner JS. 2002. Changes in mitochondrial DNA as a marker of nucleoside toxicity in HIV-infected patients. N Engl J Med 346:811–820.

Ferri KF, Jacotot E, Blanco J, Este JA, Kroemer G. 2000a. Mitochondrial control of cell death induced by HIV-1-encoded proteins. Ann N Y Acad Sci 926:149–164.

Ferri KF, Jacotot E, Blanco J, Este JA, Zamzami N, Susin SA, Xie Z, Brothers G, Reed JC, Penninger JM, Kroemer G. 2000b. Apoptosis control in syncytia induced by the HIV type 1-envelope glycoprotein complex: role of mitochondria and caspases. J Exp Med 192:1081–1092.

Hellerstein M, Hanley MB, Cesar D, Siler S, Papageorgopoulos C, Wieder E, Schmidt D, Hoh R, Neese R, Macallan D, Deeks S, McCune JM. 1999. Directly measured kinetics of circulating T lymphocytes in normal and HIV-1-infected humans. Nat Med 5:83–89.

Jacotot E, Ravagnan L, Loeffler M, Ferri KF, Vieira HL, Zamzami N, Costantini P, Druillennec S, Hoebeke J, Briand JP, Irinopoulou T, Daugas E, Susin SA, Cointe D, Xie ZH, Reed JC, Roques BP, Kroemer G. 2000. The HIV-1 viral protein R induces apoptosis via a direct effect on the mitochondrial permeability transition pore. J Exp Med 191:33–46.

Kakuda TN. 2000. Pharmacology of nucleoside and nucleotide reverse transcriptase inhibitor-induced mitochondrial toxicity. Clin Ther 22:685–708.

Lichtenstein KA, Ward DJ, Moorman AC, Delaney KM, Young B, Palella FJ Jr, Rhodes PH, Wood KC, Holmberg SD. 2001. Clinical assessment of HIV-associated lipodystrophy in an ambulatory population. AIDS 15:1389–1398.

Lim SE, Copeland WC. 2001. Differential incorporation and removal of antiviral deoxynucleotides by human DNA polymerase gamma. J Biol Chem 276:23616–23623.

Macho A, Castedo M, Marchetti P, Aguilar JJ, Decaudin D, Zamzami N, Girard PM, Uriel J, Kroemer G. 1995. Mitochondrial dysfunctions in circulating T lymphocytes from human immunodeficiency virus-1 carriers. Blood 86:2481–2487.

Macho A, Calzado MA, Jimenez-Reina L, Ceballos E, Leon J, Munoz E. 1999. Susceptibility of HIV-1-TAT transfected cells to undergo apoptosis. Biochemical mechanisms. Oncogene 18:7543–7551.

Martin JL, Brown CE, Matthews-Davis N, Reardon JE. 1994. Effects of antiviral nucleoside analogs on human DNA polymerases and

mitochondrial DNA synthesis. Antimicrob Agents Chemother 38: 2743–2749.

Martinez E, Mocroft A, Garcia-Viejo MA, Perez-Cuevas JB, Blanco JL, Mallolas J, Bianchi L, Conget I, Blanch J, Phillips A, Gatell JM. 2001. Risk of lipodystrophy in HIV-1-infected patients treated with protease inhibitors: a prospective cohort study. Lancet 357: 592–598.

Masanes F, Barrientos A, Cebrian M, Pedrol E, Miro O, Casademont J, Grau JM. 1998. Clinical, histological and molecular reversibility of zidovudine myopathy. J Neurol Sci 159:226–228.

McComsey G, Tan DJ, Lederman M, Wilson E, Wong LJ. 2002. Analysis of the mitochondrial DNA genome in the peripheral blood leukocytes of HIV-infected patients with or without lipoatrophy. AIDS 16:513–518.

Medina DJ, Tsai CH, Hsiung GD, Cheng YC. 1994. Comparison of mitochondrial morphology, mitochondrial DNA content, and cell viability in cultured cells treated with three anti-human immunodeficiency virus dideoxynucleosides. Antimicrob Agents Chemother 38:1824–1828.

Moretti S, Marcellini S, Boschini A, Famularo G, Santini G, Alesse E, Steinberg SM, Cifone MG, Kroemer G, De Simone C. 2000. Apoptosis and apoptosis-associated perturbations of peripheral blood lymphocytes during HIV infection: comparison between AIDS patients and asymptomatic long-term non-progressors. Clin Exp Immunol 122:364–373.

Moyle G. 2000. Clinical manifestations and management of antiretroviral nucleoside analog-related mitochondrial toxicity. Clin Ther 22:911–936; discussion 898.

Petit F, Arnoult D, Lelievre JD, Parseval LM, Hance AJ, Schneider P, Corbeil J, Ameisen JC, Estaquier J. 2002. Productive HIV-1 infection of primary $CD4^+$ T cells induces mitochondrial membrane permeabilization leading to a caspase-independent cell death. J Biol Chem 277:1477–1487.

Phenix BN, Lum JJ, Nie Z, Sanchez-Dardon J, Badley AD. 2001. Antiapoptotic mechanism of HIV protease inhibitors: preventing mitochondrial transmembrane potential loss. Blood 98:1078–1085.

Rasola A, Gramaglia D, Boccaccio C, Comoglio PM. 2001. Apoptosis enhancement by the HIV-1 Nef protein. J Immunol 166:81–88.

Roggero R, Robert-Hebmann V, Harrington S, Roland J, Vergne L, Jaleco S, Devaux C, Biard-Piechaczyk M. 2001. Binding of human immunodeficiency virus type 1 gp120 to CXCR4 induces mitochondrial transmembrane depolarization and cytochrome c-mediated apoptosis independently of Fas signaling. J Virol 75: 7637–7650.

Saint-Marc T, Touraine JL. 1999. The effects of discontinuing stavudine therapy on clinical and metabolic abnormalities in patients suffering from lipodystrophy. AIDS 13:2188–2189.

Saint-Marc T, Partisani M, Poizot-Martin I, Bruno F, Rouviere O, Lang JM, Gastaut JA, Touraine JL. 1999. A syndrome of peripheral fat wasting (lipodystrophy) in patients receiving long-term nucleoside analogue therapy. AIDS 13:1659–1667.

Saves M, Raffi F, Capeau J, Rozenbaum W, Ragnaud JM, Perronne C, Basdevant A, Leport C, Chene G. 2002. Factors related to lipodystrophy and metabolic alterations in patients with human immunodeficiency virus infection receiving highly active antiretroviral therapy. Clin Infect Dis 34:1396–1405.

Shikuma CM, Hu N, Milne C, Yost F, Waslien C, Shimizu S, Shiramizu B. 2001. Mitochondrial DNA decrease in subcutaneous adipose tissue of HIV-infected individuals with peripheral lipoatrophy. AIDS 15:1801–1809.

White AJ. 2001. Mitochondrial toxicity and HIV therapy. Sex Transm Infect 77:158–173.

Zaera MG, Miro O, Pedrol E, Soler A, Picon M, Cardellach F, Casademont J, Nunes V. 2001. Mitochondrial involvement in antiretroviral therapy-related lipodystrophy. AIDS 15:1643–1651.

ACADEMIC PRESS

Available online at www.sciencedirect.com

SCIENCE DIRECT®

Biochemical and Biophysical Research Communications 302 (2003) 489–495

BBRC

www.elsevier.com/locate/ybbrc

# Inhibitory and enhancing effects of insertion of central polypurine tract sequence on gene expression with vectors derived from human immunodeficiency virus type 1

Ryuta Sakuma,[a,b] Noriko Kobayashi,[a,b] Keisuke Ae,[a,b,c] and Yoshihiro Kitamura[a,b,*]

[a] *Division of Infectious Diseases, Advanced Clinical Research Center, Institute of Medical Science, University of Tokyo, 4-6-1 Shirokanedai, Minato-ku, Tokyo 108-8639, Japan*

[b] *Division of Molecular Genetics, National Institute of Infectious Diseases, 4-7-1 Musashimurayama, Tokyo 208-0011, Japan*

[c] *Section of Orthopedic Spinal Surgery, Department of Frontier Surgical Therapeutics, Division of Advanced Therapeutical Sciences, Graduate School Tokyo Medical and Dental University, 1-5-45 Yushima, Bunkyo-ku, Tokyo 113-8549, Japan*

Received 3 February 2003

**Abstract**

Reportedly, in human immunodeficiency virus type 1 (HIV) vectors, insertion of central polypurine tract (cPPT) increased expression of transgenes for a short period. To test this for a stable condition, we constructed a series of vectors carrying a *Neo*$^r$ gene as a stable marker driven by a synthetic thymidine kinase (hTK) promoter. Transduction efficiency was increased in about 2-fold and decreased in about 8-fold by insertion of the reported 178 bp and our 282 bp cPPTs, respectively. PCR analyses revealed that insertion of 282 bp cPPT, but not 178 bp cPPT, impaired integration, although it did not deteriorate nuclear transport much. Furthermore, we found that insertion of 282 bp cPPT between hTK promoter and an upstream LTR sequence reduced reporter gene activity in about 5-fold. This inhibitory effect of 282 bp cPPT may partly account for the observed decrease in transduction efficiency. We suggest that actual effect of cPPT insertion should be examined in each HIV vector.


*Keywords:* Human immunodeficiency virus type 1; Central polypurine tract; Central termination sequence; Lentivirus vector; Enhancer; Polyomavirus

In the replication of human immunodeficiency virus type 1 (HIV), the viral genomic RNA is converted to double-stranded DNA by viral reverse transcriptase [1]. In this reverse transcription, the positive-strand DNA is synthesized as two discrete overlapping segments [2,3]. The synthesis of the upstream segment starts at the 3′ polypurine tract (PPT) [2,4,5] and ends at the central termination sequence [6,7]. The synthesis of the downstream segment starts at the central PPT (cPPT) [8], which is located at about 100 nucleotides upstream of the central termination sequence. As a result, plus strand overlapping, termed DNA flap, about 100 nucleotides long occurs at the cPPT region [9]. Silent mutations that prevented the formation of the DNA flap were found to result in the decrease of the infectivity of HIV [8,10]. Reportedly, insertion of cPPT increased the transduction efficiency with some HIV vectors [11–13]. Zennou et al. [12] produced HIV vectors carrying cPPT and a GFP gene, and showed that this insertion increased the transduction with those HIV vectors. Moreover, they showed that insertion of cPPT increased the efficiency of nuclear import of viral DNA in cultured cells [12] and the transduction efficiency in rat brain using the same vectors [13]. However, a recent paper described a contrary observation that insertion of cPPT was involved in integration, but not nuclear transport, of HIV viruses [14].

There are two problems that remained to be examined, one is the effect of insertion of cPPT on the efficiency of *stable* transduction with HIV vectors, and the other is the effect of inserted cPPT on the transcription of transgenes when HIV vector DNA is integrated into

* Corresponding author. Fax: +81-35-449-5427.
*E-mail address:* yochan@ims.u-tokyo.ac.jp (Y. Kitamura).

0006-291X/03/$ - see front matter © 2003 Elsevier Science (USA). All rights reserved.
doi:10.1016/S0006-291X(03)00212-2

the host chromosome, because gene therapy requires vectors that not only introduce therapeutic gene to cells efficiently but also express them for a longer period. To examine whether HIV vectors with cPPT introduce genes more efficiently than those without cPPT, we constructed a series of HIV vectors carrying a *neomycin-resistance* (*Neo*$^r$) gene as a stable selection marker with or without cPPT in the sense or reverse orientation. To test the transduction efficiency with them, the number of G418-resistant colonies was used as an index of stable transduction. Furthermore, to test whether an upstream cPPT sequence influences the levels of expression of downstream genes in the context of a provirus, we designed a system that utilized a series of expression plasmids that expressed a *Renilla luciferase* gene under the control of heterologous promoters with or without an upstream cPPT.

## Materials and methods

*Cells.* We maintained HeLa [15] and 293T [16] cells in Dulbecco's modified Eagle's medium (DMEM) (Sigma, St. Louis, MO) supplemented with 10% fetal bovine serum (Life Technologies, Rockville, MD) and 50 μg/ml kanamycin (Sigma).

*Construction of plasmids.* We digested pLAI [17] with *Eco*RI and *Bsm*FI to obtain 282 bp cPPT fragment of HIV-$1_{LAI}$ (Fig. 1A). We made the end of this fragment blunt with DNA blunting kit (Takara Shuzo, Kyoto, Japan) and inserted it into the *Sma*I site of pBluescript II KS(−) (Stratagene, La Jolla, CA)to obtain pBS-282cPPT. We made a shorter cPPT fragment (178 bp, Fig. 1A) by polymerase chain reaction (PCR) with primers previously described [12] and cloned in pGEM-T vector (Promega, Madison, WI) to obtain pGEM-178cPPT.

We chose pHXN [18,19] as a parental provirus. As shown in Fig. 1B, the HXN vector lack structured genes (*gag*/*pol* and *env*) as well as cPPT, and carries a hybrid thymidine kinase (hTK) promoter, a *Neo*$^r$ gene, the packaging signal (Ψ), a pair of LTRs at the 5′- and 3′-ends,

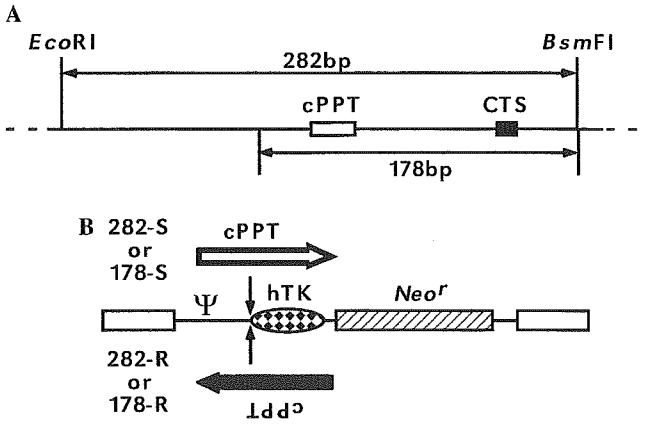


Fig. 1. Schematic representation of cPPT and HXN vectors. (A) Schematic representation of two cPPT fragments spanning the cPPT region. A horizontal line with open (cPPT) and closed (CTS) boxes stands for HIV (LAI strain) cDNA. (B) The HXN vector carries the hTK promoter (dotted oval) and a *Neo*$^r$ gene (hatched box) between 5′- and 3′-LTRs (open boxes). We inserted cPPT, either 282 or 178 bp long, of $HIV_{LAI}$ just upstream of the promoter in the sense (open arrow, HXN282-S or 178-S) or reverse (closed arrow, HXN282-R or 178-R) orientation. These figures are not drawn proportionally.

the primer binding site, and the 3′PPT. The hTK promoter contained a herpes simplex virus minimal TK promoter (127 bp, mTK) and a tandem repeat of the enhancers of polyomavirus [20]. We annealed two oligonucleotides, SN-S (5′-TCG ACA GCT GCG CCG GCG-3′) and SN-AS (5′-TCG ACA GCT GCG CCG GCG-3′), to obtain a short double-stranded adaptor that contained *Not*I and *Sal*I sites. We inserted this adaptor into the *Hin*dIII site of pHXN in either orientation. We named the plasmids that have the fragment in the sense (5′-*Sal*I–*Not*I-3′) and reverse (5′-*Not*I–*Sal*I-3′) orientation as pHXN-SN and pHXN-NS, respectively. To obtain a longer cPPT fragment, we digested pBS-282cPPT with *Not*I and *Sal*I. We inserted this 282 bp fragment between the *Not*I and *Sal*I sites of pHXN-SN and pHXN-NS, and named them pHXN282-S and pHXN282-R, respectively. pHXN282-S and pHXN282-R carried 282 bp cPPT in the sense and reverse orientation, respectively. Similarly, we excised out a shorter version of cPPT from pGEM-178cPPT with *Not*I and *Sal*I, and inserted it into pHXN-SN and pHXN-NS to obtain pHXN178-S and pHXN178-R that carried 178 bp cPPT in the sense and reverse orientation, respectively.

pRL-TK, pRL-SV40, and pRL-CMV (Promega, Madison, WI) carry a *Renilla luciferase* (Ren) gene under the control of TK promoter (753 bp), Simian Virus 40 (SV40) early promoter, and cytomegalovirus (CMV) early promoter, respectively. pGL3 (Promega) carries *Firefly luciferase* (FF) gene under the control of SV40 promoter. We used pGL3 as a control plasmid for normalization of transfection efficiency. To generate pRL-hTK carrying an hTK promoter and a *Ren* gene, we replaced the *Bgl*II–*Mlu*I fragment of pRL-TK with *Bgl*II–*Mlu*I fragment of pHXN.

To generate reporter plasmids with cPPT (282 bp), we inserted the blunted *Not*I–*Sal*I fragment of pBS-282cPPT into the *Bgl*II sites, upstream of promoters, of pRL-TK, pRL-hTK, pRL-SV40, and pRL-CMV in the sense orientation to generate pRL-S-TK, pRL-S-hTK, pRL-S-SV40, and pRL-S-CMV, respectively. We inserted the blunted *Not*I–*Sal*I fragment of pBS-282cPPT into the *Bgl*II sites of pRL-TK, pRL-hTK, pRL-SV40, and pRL-CMV in the reverse orientation to generate pRL-R-TK, pRL-R-hTK, pRL-R-SV40, and pRL-R-CMV, respectively. We inserted the blunted *Bss*HII–*Kpn*I fragment of pHXN into the *Bgl*II sites, just upstream of promoters, of pRL-TK, pRL-S-TK, pRL-R-TK, pRL-hTK, pRL-S-hTK, and pRL-R-hTK, to generate pRL-LTK, pRL-S-LTK, pRL-R-LTK, pRL-LhTK, pRL-S-LhTK, and pRL-R-LhTK, respectively.

*Production of HIV vectors.* We produced HIV vectors pseudotyped with the vesicular stomatitis virus G protein. The $pCAGP_{LAI}\Delta B$, in which the *env* region between the two *Bgl*II sites was deleted from pCAGP [18], was used to supply *gag* and *pol* gene products. The day before transfection, we spread $1 \times 10^6$ of 293T cells in a 60-mm dish. We transfected cells with 1 μg pHXN, or one of its derivatives described above, together with 1 μg each of $pCAGP_{LAI}\Delta B$ and pMD.G. [21] in 20 μl of LipofectAMINE 2000 (Life Technologies), to generate HXN vector or its derivatives, respectively. Forty-eight hours after transfection, we collected culture supernatants and filtered them through 0.45-μm filters (Millipore, Bedford, MA). Then, we treated these supernatants with 500 units per ml of DNase I (Takara Shuzo) at 37 °C for an hour and stored at −80 °C.

*Determination of amounts of p24.* We assayed the amount of p24 in the culture supernatant with a p24 specific enzyme-linked immunosorbent assay kit (Dainabot, Tokyo, Japan), according to manufacturer's instruction.

*Vector titration.* The day before infection, we spread $5 \times 10^5$ HeLa cells in a 35-mm dish. We infected cells for 8 h with 1 ml of an HIV vector equivalent to 1 ng of p24. Twenty-four hours after infection, we spread those cells in a 100-mm dish. The next day, we began to select them with 1 mg/ml G418 (Sigma) and continued this selection for 2 weeks. We described titers of HIV vectors as colony forming units (CFU) per 1 ng of p24.

*Assay of vector RNA.* We extracted viral RNA from each vector supernatant equivalent to 10 ng p24 with ISOGEN (Nippon Gene,

Tokyo, Japan), according to manufacturer's instruction. To convert the viral RNA to DNA, we treated it with ReverTra Ace (Toyobo, Osaka, Japan), according to manufacturer's instruction. We amplified the LTR fragment by PCR (denaturation at 96 °C for 10 s, annealing at 55 °C for 15 s, and extension at 72 °C for 2 min, 30 cycles) using 5NC2 (5′-CCG AGT CCT GCG TCG AGA GAG C-3′) and LTR5 (5′-GGC TAA CTA GGG AAC CCA CTG CTT-3′) primers [21].

*Detection of the 2-LTR junction.* The day before infection, we spread $5 \times 10^5$ HeLa cells in a 35-mm dish. We infected cells with 1 ml HIV vector equivalent to 50 ng p24 for 16 h. We extracted the total cellular DNA with SmiTEST R&D (Genome Science Laboratory, Fukuoka, Japan). We amplified 2-LTR fragment by PCR (denaturation at 96 °C for 10 s, annealing at 55 °C for 15 s, and extension at 72 °C for 2 min, 30 cycles) using 2LTR-F (5′-GCC TCA ATA AAG CTT GCC TTG-3′) and 2LTR-R (5′-TCC CAG GCT CAG ATC TGG TCT AAC-3′) primers. Then, we amplified the internal region of the PCR products by nested-PCR (denaturation at 96 °C for 10 s, annealing at 55 °C for 15 s, and extension at 72 °C for 2 min, 45 cycles) using 2LTR-FF (5′-GAT CCC TCA GAC CCT TTT AG-3′) and 2LTR-RR (5′-CCC AGT ACA GGC AAA AAG CAG-3′) primers.

*Detection of integrated vectors by Alu-PCR.* Quantitative assay for integrated HIV was carried out as described by Chun et al. with a minor modification. Briefly, we infected HeLa cells ($1 \times 10^5$ cells/35-mm dish) with vectors (p24 equivalent to 10 ng) whose cellular DNA was subjected to PCR. The sequences of the amplification primers were as follows: genomic *Alu* forward, 5′-TCC CAG CTA CTC GGG AGG CTG AGG-3′; and HIV LTR reverse, 5′-AGG CAA GCT TTA TTG AGG CTT AAG C-3′. Reactions were carried out in 50 μl of 1× Ex-*Taq* buffer containing 0.2 mM each of dNTPs, 200 nM *Alu* forward primer, 200 nM LTR reverse primer, and 1.25 U Ex-*Taq* DNA polymerase (Takara Shuzo). The thermal cycler (ABI9700; Perkin–Elmer, Wellesley, MA) was programmed to perform a 3-min hot start at 94 °C, followed by 22 cycles of denaturation at 94 °C for 30 s, annealing at 66 °C for 30 s, and extension at 72 °C for 10 min. Following the initial PCR, by using an aliquot equivalent to 1/400 of the initial PCR product, a second nested PCR was carried out in 50 μl of 1× Ex-*Taq* buffer containing 0.2 mM each of dNTPs, 200 nM each of LTR forward and reverse primers, and 1.25 U Ex-*Taq* DNA polymerase. The sequences of the primers were as follows: NI-25, 5′-CAC ACA CAA GGC TAC TTC CCT-3′ and NI-23, 5′-GCC ACT CCC CIG TCC CGC CC-3′. The thermal program was 3-min hot start at 94 °C, followed by 29 cycles of denaturation at 95 °C for 30 s, annealing at 63 °C for 30 s, and extension at 72 °C for 1 min. PCR products were analyzed by gel electrophoresis followed by Southern blot/hybridization by using $^{32}$P 5′-labeled probes (NI probe 5′-GGA TGG TGC TTC AAG ITA GTA CC-3′). After Southern blot hybridization, bands were quantified with an image analyzer, BAS2000 (Fuji Film, Tokyo, Japan).

*Dual luciferase reporter assay.* The day before transfection, we spread $3 \times 10^4$ of 293T cells in a well of a 96-well plate. We transfected cells with 40 ng of one of the pRL-derived plasmids together with 40 ng of pGL3 (Promega) in LipofectAMINE PLUS (Life Technologies). Forty-eight hours after transfection, we assayed both Ren and FF activities with the Dual luciferase reporter assay kit (Promega), according to manufacturer's instruction. We normalized a Ren with the FF activities of the same sample.

## Results

### *Insertion of cPPT increased the amount of HXN vectors released in the supernatants*

We transfected 293T cells with pHXN, pHXN282-S, pHXN282-R, pHXN178-S, or pHXN178-R plasmid together with helper plasmids, to produce HXN, HXN282-S, HXN282-R, HXN178-S, or HXN178-R vector, respectively, pseudotyped with vesicular stomatitis virus G proteins. We assayed the amount of p24 and viral RNA released in each supernatant and found that the amounts of p24 released from the 293T cells transfected with pHXN-derived plasmids with cPPT of either 282 or 178 bp were increased in about 3–5-fold (Fig. 2A). Moreover, we quantitated the amount of RNA of the vectors normalized with the amount of p24 by Northern blot analysis. We found that the amount of viral RNA per p24 of all the vector samples was almost the same as that in HXN vector (data not shown). We concluded that the transfection of 293T cells with HIV vectors with cPPT, either 178 or 282 bp long, produced more vector particles

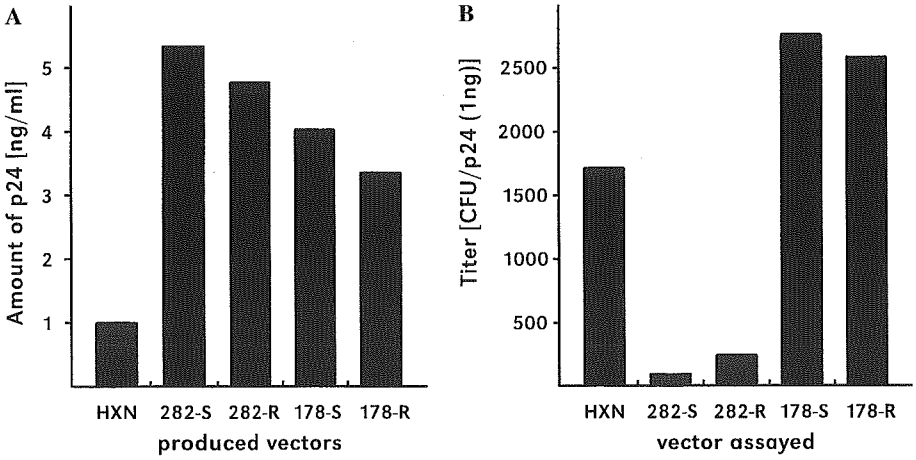


Fig. 2. Comparison of two cPPT fragments. (A) cPPT's effect on the production of HXN-derived vectors.We transfected 293T cells with the indicated plasmid together with helper plasmids. Forty-eight hours after transfection, we assayed the amount of p24 in the culture supernatant of transfected 293T cells by ELISA. (B) cPPT's effect on infectivity of HXN-derived vectors.We infected HeLa cells with the indicated vectors and selected infected cells with G418 for 2 weeks, and showed the results as colony forming units (CFU) per 1 ng of p24.

than those without cPPT independently of the orientation of the inserted cPPT fragment.

*Opposite effect of insertion of longer and shorter cPPTs on the titers of the vectors*

We examined the infectivity of the produced HIV vectors. We infected HeLa cells with supernatants obtained from 293T cells transfected with one of the pHXN-derived plasmids, and selected them with G418 to obtain transduced cells. The infectivity was figured out by the number of G418-resistant colonies per 1 ng of p24. The infectivity of HXN282-S and HXN282-R was about eight times lower than that of HXN (Fig. 2B). In contrast, the infectivity of HXN178-S and HXN178-R was 1.5–2 times higher than that of HXN (Fig. 2B). Insertion of a longer cPPT decreased the infectivity of vectors independently of the orientation of insertion.

To confirm that this low infectivity was due to decreased integration, we measured integration by Alu-PCR followed by Southern blot analysis of the amplified products [22]. This technique allowed us to measure the average amount of DNA of integrated proviruses. We found that the integrated DNA amount of HXN282-S or -R was decreased to less than 10% of that of HXN at any time points (8, 16, or 24 h after infection; Fig. 3). In contrast, the integrated DNA amount of HXN178-S or -R was not decreased compared to that of HXN at any time point (8, 16, or 24 h after infection; Fig. 3).

We examined whether this decrease in integration activity of HXN282-S and -R was ascribable to low nuclear import of the vector DNA or due to low activity of post-entry events. We monitored the nuclear import of vector DNA by detecting the circular form of vector

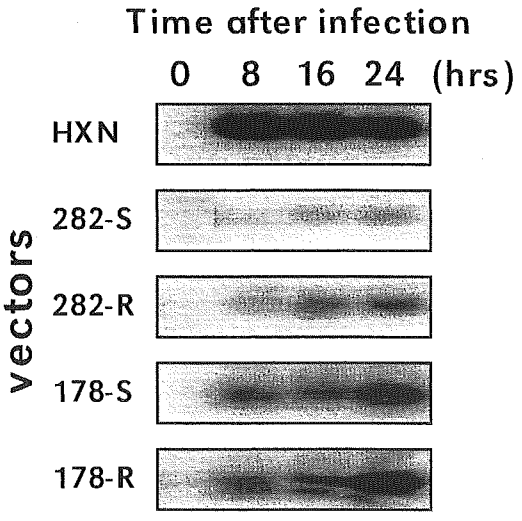


Fig. 3. Integration analyzed by Alu-LTR PCR. We extracted cellular DNA 0, 8, 16, and 24 h after infection, amplified *Alu*-LTR junction by nested PCR, and detected the bands by Southern blot/hybridization. A typical result is shown.

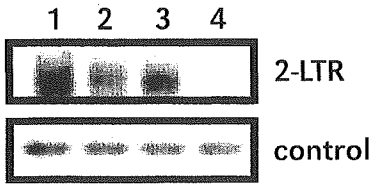


Fig. 4. Infectivity of HXN-derived vectors. We extracted cellular DNA 16 h after infection and amplified 2-LTR junction by nested PCR (upper panel) and a region of a *β-globin* gene as control (lower panel). Lane 1, HXN; lane 2, HXN282-S; lane 3, HXN282-R; and lane 4, mock infected.

DNA with two LTRs, because those molecules are characteristic to and indicators of nuclear import of vector DNA [23]. We amplified a 2-LTR junction by semi-quantitative nested PCR with total cellular DNA from infected HeLa cells. Insertion of cPPT in HXN did not significantly affect the amount of 2-LTR junction in cells infected with HXN282-S or HXN282-R (Fig. 4, compare lanes 2 and 3 to lane 1). We concluded that insertion of cPPT decreased the integration activity without much affecting nuclear import of vector DNA. That is, insertion of cPPT is likely to impair an uncharacterized post-nuclear entry event that enables imported DNA to be permissive for integration in cell nuclei at least in our system.

*Insertion of cPPT increased transient expression*

Hoping to know whether the decrease in infectivity with 282 bp cPPT was ascribed partly to impairment in post-integration events including transcription of a transgene in the context of provirus, we designed an expression assay system. As shown in Fig. 5A, we constructed a series of pRL plasmids by mimicking proviral structures: these plasmids had expression cassettes containing an internal promoter (SV40, CMV, TK, or hTK) and *Ren* gene with or without an upstream LTR. cPPT (282 bp) were introduced upstream of the internal promoter in the sense or reverse orientation. Without an LTR, insertion of cPPT resulted in increase of the Ren activity. For example, the Ren activity in cells transfected with pRL-S-TK or pRL-R-TK was about 2-fold higher than that with pRL-TK. In experiments with hTK (pRL-hTK, pRL-S-hTK, and pRL-R-hTK), SV40 (pRL-SV40, pRL-S-SV40, and pRL-R-SV40), and CMV (pRL-CMV, pRL-S-CMV, and pRL-R-CMV) promoters, we obtained results similar to those with the TK promoter (Fig. 5B). With an upstream LTR, the Ren activity in cells transfected with pRL-S-LTK or pRL-R-LTK was almost the same as that with the pRL-LTK. On the contrary, the Ren activity in cells transfected with pRL-S-LhTK or pRL-R-LhTK was about 5-fold lower than that with pRL-LhTK independently of the orientation of the inserted cPPT. Taking these altogether, we concluded that a special combination of

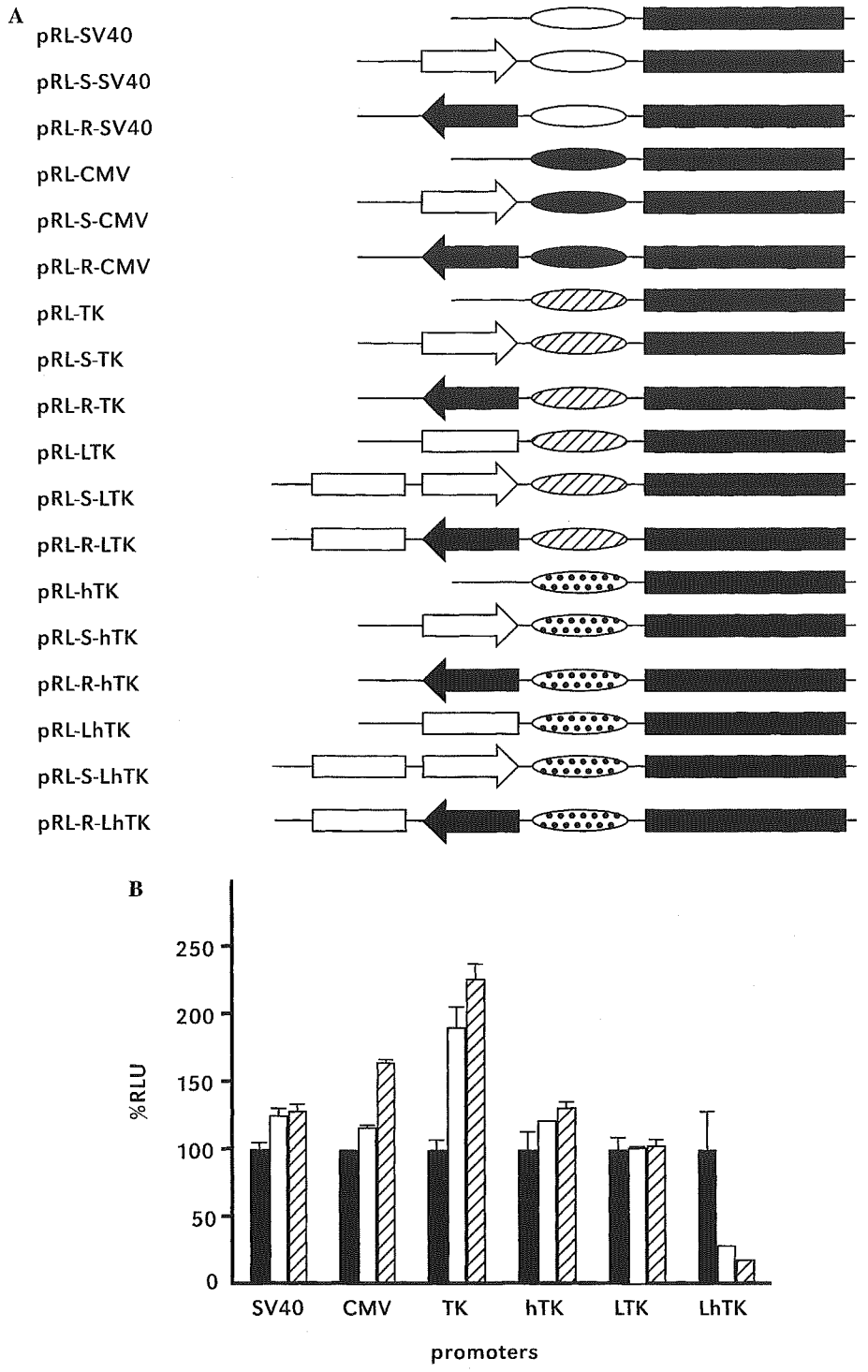


Fig. 5. Effect of inserted cPPT on the expression of a downstream *Renilla luciferase* gene. (A) We constructed plasmids carrying cPPT and LTR. These reporter plasmids contain an SV40 early promoter (open ovals), a CMV promoter (closed ovals), a TK promoter (hatched ovals), or an hTK promoter (dotted ovals), together with a downstream Ren cDNA (closed boxes). These plasmids contain cPPT in a sense (open arrows) or reverse (closed arrows) orientation upstream of each promoter. Some reporter plasmids contain LTR (open boxes) of HIV-$1_{LAI}$ upstream of promoter or cPPT. The figures are not drawn proportionally. (B) We transfected 293T cells with one of these reporter plasmids together with pGL3, a control plasmid for normalization of transfection efficiency. Forty-eight hours after transfection, we assayed both Ren and FF activities of transfected 293T cells. We normalized Ren with FF activities of samples; the value of Ren activity was divided with the value of FF. Then, we described the activity of reporter plasmid carrying cPPT in the sense (open bars) or reverse (hatched bars) orientation as a percentage of the activity obtained from 293T cells transfected with reporter plasmid without cPPT (closed bars). Results are from three independent experiments and shown as averages with standard deviation.

an upstream LTR, cPPT, and downstream hTK decreased Ren activity independently of the orientation of the inserted cPPT. This may contribute decreased titers of HXN vectors carrying 282 bp cPPT.

## Discussion

We found that insertion of our 282 bp but not the original 178 bp cPPT decreased transduction efficiency with HIV vector carrying a *Neo*$^r$ gene and both enhanced the production of vector particles. Evidence that the insertion decreased transduction efficiency with *Neo*$^r$ gene is that the insertion decreased the number of G418-resistant colonies in about 8-fold (Fig. 2B). This insertion resulted in decreased integration activity (Fig. 3) without much affecting the efficiency of nuclear import of HIV vector DNA very much (Fig. 4). Evidence that the insertion enhanced vector particle production is that the amount of p24 released in the supernatants of 293T cells transfected with pHXN282/178-S or pHXN282/278-R was more than that of pHXN-transfected cells (Fig. 2A), and that vector RNAs in the HXN-S and HXN-R vectors were almost as abundant as the amount in the HXN vector (data not shown).

Furthermore, we found that insertion of the 282 bp cPPT upstream of heterologous promoter enhanced the expression of a downstream gene independently of the orientation of the inserted cPPT. Evidence that the insertion of cPPT (282 bp) enhanced the expression of a gene is that, in a transient expression assay using a luciferase gene as a reporter, the insertion in upstream of heterologous promoters (TK, SV40, and CMV promoters) enhanced transient expression of a downstream *Ren* gene (Fig. 4). To our knowledge, this is the first report about an enhancing effect of cPPT on gene expression.

Our data disagreed with previous reports that the insertion of cPPT increased the efficiency of transduction with HIV vectors [12,13,24,25]. What made the difference? First, they used the GFP gene as a *transient* marker, while we use *Neo*$^r$ gene as a *stable* marker. Second, they used internal CMV promoter with 178 bp cPPT fragment, while we used hTK promoter with 282 bp cPPT fragment. Finally, Rev-responsible element and splice-acceptor sequence were included in their vectors but not ours. An obvious factor for the low transduction efficiency is difference between two cPPTs (282 bp vs. 178 bp); insertion of cPPT (282 bp) but not cPPT (178 bp) significantly decreased integration of HXN vectors by an unknown mechanism (Fig. 3). Another likely factor that accounts for the discrepancy seems to be the hTK promoter that we used. We found that, in the context of [LTR-hTK-Ren], insertion of cPPT between the LTR and hTK decreased Ren expression. In contrast, we observed that, in the context of [LTR-TK-Ren], insertion of cPPT between the LTR and TK increased Ren expression. Taking these together, we suppose that unknown sequence present in hTK but absent in TK may account for the results. This inhibitory function of hTK in combination with LTR and cPPT may partly contribute to the observed reduction in transduction efficiency.

Contrary to this discrepancy, our results are exactly consistent with observations of a recent paper [14]. Using HIV viruses with mutations in cPPT region, they decribed that cPPT was not essential for nuclear import of viral cDNA but increased integration efficiency modestly. They suggested that cPPT is involved in an uncharacterized post-nuclear entry event rather than the nuclear import. Since insertion of cPPT into HIV-1 vectors does not always increase their gene transduction efficiency, we suggest that an enhancing/inhibitory effect of the cPPT insertion should be examined in each vector to obtain better HIV vectors. We speculate that the enhancing effect of cPPT likely requires (i) an optimal site of insertion within vectors, (ii) optimal promoter/gene partners, (iii) other miscellaneous cis-acting sequences like the Rev-responsible element, and/or (iv) an optimal length of vectors. Actually, insertion of a shorter cPPT did not decrease titers of the vector in our system.

## Acknowledgments

We thank Dr. Takashi Shimada (Nippon Medical College) for pHXN and pCAGP. We thank Dr. Didier Trono (University of Geneva) for pMD.G. We are grateful to Tadahito Kanda (NIID) and Kunito Yoshiike (National Institute of Health, Thailand) for critical reading of the manuscript. This work was partly supported by grants to YK from the Ministry of Health, Labor and Welfare of Japan, the Japan Human Sciences Foundation, and the Ministry of Education, Culture, Sports, Science and Technology of Japan.

## References

[1] E.J. Arts, S.F. Le Grice, Interaction of retroviral reverse transcriptase with template-primer duplexes during replication, Prog. Nucleic Acid Res. Mol. Biol. 58 (1998) 339–393.
[2] O. Hungnes, E. Tjotta, B. Grinde, The plus strand is discontinuous in a subpopulation of unintegrated HIV-1 DNA, Arch. Virol. 116 (1991) 133–141.
[3] Y. Quan, L. Rong, C. Liang, M.A. Wainberg, Reverse transcriptase inhibitors can selectively block the synthesis of differently sized viral DNA transcripts in cells acutely infected with human immunodeficiency virus type 1, J. Virol. 73 (1999) 6700–6707.
[4] P. Charneau, F. Clavel, A single-stranded gap in human immunodeficiency virus unintegrated linear DNA defined by a central copy of the polypurine tract, J. Virol. 65 (1991) 2415–2421.
[5] M.D. Powell, J.G. Levin, Sequence and structural determinants required for priming of plus-strand DNA synthesis by the human immunodeficiency virus type 1 polypurine tract, J. Virol. 70 (1996) 5288–5296.
[6] P. Charneau, G. Mirambeau, P. Roux, S. Paulous, H. Buc, F. Clavel, HIV-1 reverse transcription. A termination step at the center of the genome, J. Mol. Biol. 241 (1994) 651–662.

[7] M. Lavigne, P. Roux, H. Buc, F. Schaeffer, DNA curvature controls termination of plus strand DNA synthesis at the centre of HIV-1 genome, J. Mol. Biol. 266 (1997) 507–524.
[8] P. Charneau, M. Alizon, F. Clavel, A second origin of DNA plus-strand synthesis is required for optimal human immunodeficiency virus replication, J. Virol. 66 (1992) 2814–2820.
[9] L. Hameau, J. Jeusset, S. Lafosse, D. Coulaud, E. Delain, T. Unge, T. Restle, E. Le Cam, G. Mirambeau, Human immunodeficiency virus type 1 central DNA flap: dynamic terminal product of plus-strand displacement DNA synthesis catalyzed by reverse transcriptase assisted by nucleocapsid protein, J. Virol. 75 (2001) 3301–3313.
[10] O. Hungnes, E. Tjotta, B. Grinde, Mutations in the central polypurine tract of HIV-1 result in delayed replication, Virology 190 (1992) 440–442.
[11] M. Stevenson, HIV nuclear import: What's the flap? Nat. Med. 6 (2000) 626–628.
[12] V. Zennou, C. Petit, D. Guetard, U. Nerhbass, L. Montagnier, P. Charneau, HIV-1 genome nuclear import is mediated by a central DNA flap, Cell 101 (2000) 173–185.
[13] V. Zennou, C. Serguera, C. Sarkis, P. Colin, E. Perret, J. Mallet, P. Charneau, The HIV-1 DNA flap stimulates HIV vector-mediated cell transduction in the brain, Nat. Biotechnol. 19 (2001) 446–450.
[14] J.D. Dvorin, P. Bell, G.G. Maul, M. Yamashita, M. Emerman, M.H. Malim, Reassessment of the roles of integrase and the central DNA flap in human immunodeficiency virus type 1 nuclear import, J. Virol. 76 (2002) 12087–12096.
[15] W.F. Scherer, J.T. Syverton, G.O. Gey, Studies on the propagation in vitro of poliomyelitis viruses IV. Viral multiplication in a stable strain of human malignant epithelial cells (strain HeLa) derived from an epidermoid carcinoma of the cervix, J. Exp. Med. 97 (1953) 695.
[16] F.L. Graham, J. Smiley, W.C. Russell, R. Nairn, Characteristics of a human cell line transformed by DNA from human adenovirus type 5, J. Gen. Virol. 36 (1977) 59–74.
[17] K. Peden, M. Emerman, L. Montagnier, Changes in growth properties on passage in tissue culture of viruses derived from infectious molecular clones of HIV-1LAI, HIV-1MAL, and HIV-1ELI, Virology 185 (1991) 661–672.
[18] T. Shimada, H. Fujii, H. Mitsuya, A.W. Nienhuis, Targeted and highly efficient gene transfer into CD4+ cells by a recombinant human immunodeficiency virus retroviral vector, J. Clin. Invest. 88 (1991) 1043–1047.
[19] Y. Kitamura, T. Ishikawa, N. Okui, N. Kobayashi, T. Kanda, T. Shimada, K. Miyake, K. Yoshiike, Inhibition of replication of HIV-1 at both early and late stages of the viral life cycle by single-chain antibody against viral integrase, J. Acquir. Immune Defic. Syndr. Hum. Retrovirol. 20 (1999) 105–114.
[20] K.R. Thomas, M.R. Capecchi, Site-directed mutagenesis by gene targeting in mouse embryo-derived stem cells, Cell 51 (1987) 503–512.
[21] L. Naldini, U. Blomer, P. Gallay, D. Ory, R. Mulligan, F.H. Gage, I.M. Verma, D. Trono, In vivo gene delivery and stable transduction of nondividing cells by a lentiviral vector, Science 272 (1996) 263–267.
[22] T.W. Chun, L. Stuyver, S.B. Mizell, L.A. Ehler, J.A. Mican, M. Baseler, A.L. Lloyd, M.A. Nowak, A.S. Fauci, Presence of an inducible HIV-1 latent reservoir during highly active antiretroviral therapy, Proc. Natl. Acad. Sci. USA 94 (1997) 13193–13197.
[23] C.D. Pauza, P. Trivedi, T.S. McKechnie, D.D. Richman, F.M. Graziano, 2-LTR circular viral DNA as a marker for human immunodeficiency virus type 1 infection in vivo, Virology 205 (1994) 470–478.
[24] A. Sirven, E. Ravet, P. Charneau, V. Zennou, L. Coulombel, D. Guetard, F. Pflumio, A. Dubart-Kupperschmitt, Enhanced transgene expression in cord blood CD34(+)-derived hematopoietic cells, including developing T cells and NOD/SCID mouse repopulating cells, following transduction with modified trip lentiviral vectors, Mol. Ther. 3 (2001) 438–448.
[25] V. Dardalhon, B. Herpers, N. Noraz, F. Pflumio, D. Guetard, C. Leveau, A. Dubart-Kupperschmitt, P. Charneau, N. Taylor, Lentivirus-mediated gene transfer in primary T cells is enhanced by a central DNA flap, Gene Ther. 8 (2001) 190–198.

JOURNAL OF VIROLOGY, Jan. 2003, p. 1589–1594 Vol. 77, No. 2
0022-538X/03/$08.00+0 DOI: 10.1128/JVI.77.2.1589–1594.2003


# Proline 78 Is Crucial for Human Immunodeficiency Virus Type 1 Nef To Down-Regulate Class I Human Leukocyte Antigen

Takeshi Yamada,[1]† Naotoshi Kaji,[1,2] Takashi Odawara,[1] Joe Chiba,[2] Aikichi Iwamoto,[1,3] and Yoshihiro Kitamura[1]*

*Division of Infectious Diseases, Advanced Clinical Research Center,[1] and Department of Infectious Disease and Applied Immunology, Institute of Medical Science,[3] The University of Tokyo, Tokyo 108-8639, and Department of Biological Science and Technology, Science University of Tokyo, Chiba 278-8510,[2] Japan*

Received 18 April 2002/Accepted 4 October 2002

**Human immunodeficiency virus type 1 Nef down-regulates human leukocyte antigen class I (HLA-I) in T lymphocytes, and the down-regulation involves the Nef proline-rich domain (PRD) containing four prolines at positions 69, 72, 75, and 78. We used a Sendai virus vector with *nef* and examined regulation by Nef of HLA-I and CD4 in suspension cultures of cells such as T lymphocytes. Analyses of a series of PRD substitution mutants indicated that, because the substitution of Pro78 with Ala abolished down-regulation of HLA-I but not of CD4, Pro78 is important for HLA-I down-regulation in T lymphocytes.**

Host immune responses against viral infection are mediated by cytotoxic T lymphocytes, which recognize viral antigens presented by human leukocyte antigen class I (HLA-I) molecules, encoded by the HLA-A, -B, and -C loci, on the surfaces of infected cells (13, 24). Some viruses escape host immune responses down-regulating HLA-I expression by their own proteins. Examples include K3 and K5 zinc finger membrane proteins of Kaposi's sarcoma-associated herpesvirus (KSHV) (15, 22, 26), and Nef of human immunodeficiency virus type 1 (HIV-1). Nef is a 27-kDa myristoylated protein of approximately 200 amino acids which is produced abundantly in early stages of the viral life cycle (16) and decreases the number of HLA-I and CD4 molecules on the surfaces of infected cells (2, 7, 28), protecting HIV-1-infected cells from anti-HIV-1 cytotoxic-T-lymphocyte attack (4, 5). Nef contains a characteristic proline-rich domain (PRD), which consists of four proline residues at amino acids 69, 72, 75, and 78. The PRD has been found to be involved in decreasing the number of HLA-I molecules by affecting HLA-I trafficking via interactions with protein sorting machinery (9, 20) and to bind to Src homology domain 3 (SH3 domain), with Pro72 and Pro75 but not Pro69 or Pro78, forming a binding facet (17, 19). Some assumed that SH3-binding activity contributed greatly to HLA down-regulation, while others assumed that it contributed less (6, 9, 20, 25). Since no studies on Ala substitution for each Pro have been available, it remains unclear which proline residue is the most important among the four proline residues (Pro69, Pro72, Pro75, and Pro78) for Nef to down-regulate HLA-I in T cells.

In most studies, although T lymphocytes are the main target for HIV-1, adhesion cells such as human IMR90 fibroblasts and 293 cells have been used for analysis of HLA-I down-regulation by Nef because of the general difficulty of expressing *nef* in suspended cells by transfection (9, 18). To express enough Nef for studying HLA-I down-regulation in suspended rather than adherent cells, we employed a recombinant Sendai virus (rSeV) system, which has been shown to express large amounts of heterologous recombinant proteins in 24 h after infection in both suspended and adherent cells (12, 31).

To identify which proline residue among the four in the PRD contributes most to HLA-I down-regulation, we constructed a series of rSeVs that express various Nef proteins with or without substitution of alanines for prolines. The DNA constructs used in these experiments were derived from a provirus plasmid, pNL-432 (1). Mutations were introduced into *nef* by site-directed mutagenesis based on overlap extension PCR (14). Each proline residue at amino acid 69, 72, 75, or 78 in the PRD of Nef was changed to alanine (P69A, P72A, P75A, P78A), and four consecutive glutamic acids from amino acid 62 to 65 in a highly conserved cluster of acidic residues, which is reported to bind to PACS-1 to down-regulate HLA-I (23), were changed to alanines (EEEE65AAAA). The resultant plasmids were designated pNL-432-APPP (P69A), pNL-432-PAPP (P72A), pNL-432-PPAP (P75A), pNL-432-PPPA (P78A), pNL-432-PPAA (P75A and P78A), pNL-432-PAAA (P72A, P75A, and P78A), pNL-432-PPPP/AAAA (P69A, P72A, P75A, and P78A), and pNL-432-EEEE/AAAA (EEEE65AAAA). An SeV-based expression vector, pSeV(+)18bV(−) (21), which generates antigenomic positive-strand viral RNA in which the viral V gene has been knocked out, was used in this study. The *nef* genes were amplified on wild-type and mutant pNL-432 plasmids by PCR. Based on the KSHV genomic sequence (26),

* Corresponding author. Mailing address: Division of Infectious Diseases, Advanced Clinical Research Center, Institute of Medical Science, University of Tokyo, 4-6-1 Shirokanedai, Minato-ku, Tokyo 108-8639, Japan. Phone: 81-3-5449-5336. Fax: 81-3-5449-5427. E-mail: yochan@ims.u-tokyo.ac.jp.

† Present address: Department of Microbiology, Graduate School of Medicine, The University of Tokyo, Tokyo 113-0033, Japan.

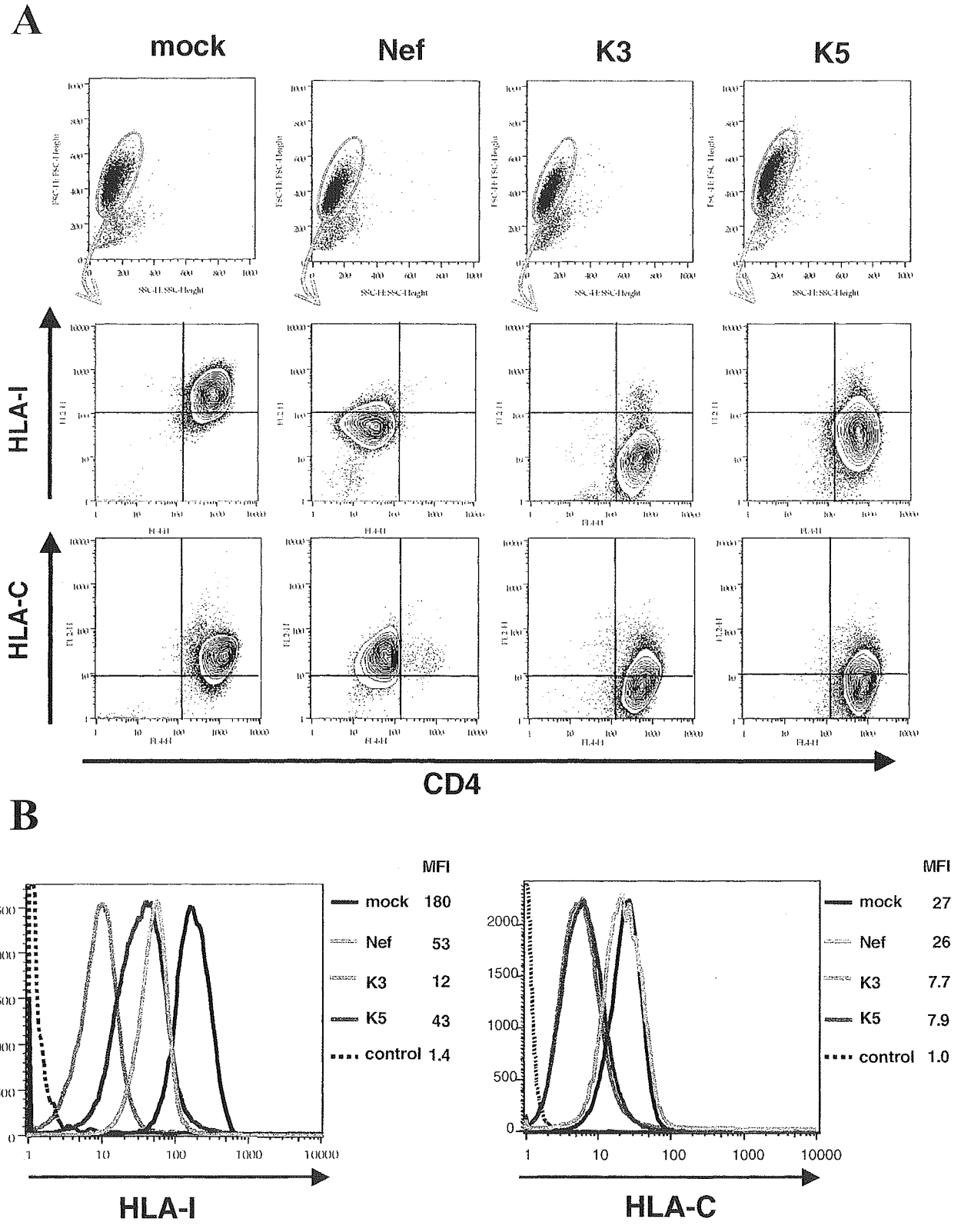


FIG. 1. Flow-cytometric analysis of CD4 and HLA-I expression on cell surfaces. CEM cells were infected with each rSeV at a multiplicity of infection of 10 for 1 h. Twenty-four hours after infection, cells were treated at 4°C for 20 min with an allophycocyanin-labeled anti-CD4 antibody (Becton Dickinson Immunocytometry Systems, San Jose, Calif.), and an R-phycoerythrin-labeled anti-HLA-I antibody (W6/32; Dako, Glostrup, Denmark) against a monomorphic epitope of HLA-A, -B, and -C or an anti-HLA-C antibody (29) with an R-phycoerythrin-labeled secondary antibody (Dako). A FACSCalibur flow cytometer (Becton Dickinson Immunocytometry Systems) with CellQuest software (Becton Dickinson Immunocytometry Systems) was used for flow cytometry. Isotype-matched control antibodies were included to detect nonspecific binding to cells.

we amplified DNA containing the KSHV K3 and K5 open reading frames from genomic DNA of BCBL-1 cells (3); PCR fragments were cloned in pSeV(+)18bV(−) (27). Unexpectedly, our K3 construct lacked 33 nucleotides spanning from nucleotide 583 to 615 in K3 ORF (26). The rSeV stocks were obtained as previously described (30) and generally had infectious titers of $10^7$ to $10^9$ PFU/ml. The mutant rSeVs were designated SeV-EEEE/AAAA, SeV-APPP, SeV-PAPP, SeV-PPAP, SeV-PPPA, SeV-PPAA, SeV-PAAA, SeV-PPPP/AAAA, SeV-K3, and SeV-K5.

Nef, K3, and K5 expression significantly down-regulated surface expression of HLA-I molecules compared with the mock vector, whereas the down-regulation of CD4 molecules was observed only with Nef expression (Fig. 1A). Furthermore, HLA-C molecules were down-regulated specifically by K3 and K5 but not Nef. We found that KSHV K3 and K5 down-regulated HLA-I molecules to a lower level than Nef in terms of the mean fluorescence intensities (Fig. 1B). SeV-PPPP/AAAA abolished HLA-I down-regulation strongly compared to SeV-EEEE/AAAA (Fig. 2A). Each of the four prolines in the PRD was replaced by alanine to address the question of which of the four prolines in the PRD is most critical. CD4 on CEM cells were down-regulated by infection with SeV-APPP, -PAPP, -PPAP, or -PPPA, to an extent similar to that observed with wild-type SeV. HLA-I expression was down-regulated by SeV-APPP, -PAPP, and -PPAP at a level equivalent to that of SeV-wild, but not by SeV-PPPA. Furthermore, the PPAA, PAAA, and PPPP/AAAA mutants inhibited the down-regulation of HLA-I more than the PPPA mutant. The cell lysates infected with rSeV were analyzed by Western blotting with anti-Nef mouse monoclonal antibody (Intracel, Cambridge, Mass.). Since we observed similar expression levels of Nefs in the samples (Fig. 2B), the observed extent of down-regulation seemed to be simply a function of the nature of the introduced mutations.

To ascertain whether the effects observed with Nef alone were relevant to events taking place during HIV-1 infection, selected mutants were analyzed within the context of HIV-1-infected CEM-GFP cells. CEM-GFP cells are human T-lymphoid cells that contain an HIV-1 long terminal repeat-driven green fluorescent protein (GFP) cDNA in which GFP expression is induced by Tat (8). The CEM-GFP cell line was from the AIDS Research and Reference Reagent Program, Division of AIDS, National Institute of Allergy and Infectious Diseases, National Institutes of Health. We used CEM-GFP cells for measuring the level of HLA-I expression on HIV-1-infected cells directly. CEM-GFP cells were infected with the different HIV-1 variants by cocultivation for 48 h with transfected HeLa cells in RPMI 10, as previously described (20). As shown in Fig. 3A, in the case of wild-type virus infection, down-regulation of HLA-I expression in GFP-positive cells was observed, and the fluorescence intensity for GFP was reversely correlated with the level of HLA-I expression. In agreement with the results from analysis with rSeVs, the PPPP/AAAA mutation abolished HLA-I down-regulation strongly, compared to EEEE/AAAA. HLA-I molecules were not internalized by PPPA, although APPP, PAPP, and PPAP proteins down-regulated surface expression of HLA-I in GFP-positive cells. Furthermore, additional mutations of Pro78 of the PRD, i.e., PPAA, PAAA, and PPPP/AAAA, inhibited down-regulation of HLA-I more strongly than PPPA. By analysis of HLA-C expression, we found that HLA-C down-regulation was not induced even in the case of infection with HIV-1 carrying the wild-type *nef* gene (Fig. 3B).

Our rSeV system proved to be competent in expressing Nef in a T-cell line, CEM, and primary T cells (data not shown), since Nef expressed by rSeV was biologically functional in terms of HLA-I down-regulation. Using this system, we determined that Pro78 in the PRD contributed most to HLA-I down-regulation but not to CD4 down-regulation, in suspension-cultured cells. Evidence that rSeVs expressed biologically functional Nef is found in the fact that in both rSeV (Fig. 2A) and HIV-1 (Fig. 3A) systems, Nef down-regulated HLA-I similarly and that HLA-I-A and -B molecules were down-regulated selectively (Fig. 1B and 3B). Evidence that Pro78 played a crucial role in down-regulation of HLA-I is that rSeV-mediated introduction of mutant *nef* genes inhibited down-regulation of HLA-I but not CD4 in CEM cells (Fig. 2A) and that HIV-1 mutants showed similar results (Fig. 3A). A detailed study on HIV-1 Nef not only will lead to a better understanding of molecular mechanisms of HLA-I down-regulation but also may provide novel means for developing Nef inhibitors. The use of rSeV will significantly facilitate these analyses on Nefs.

Our results showed that Pro78 was the most critical residue for HLA-I down-regulation, while Pro72 and Pro75 were much less critical. Since the latter proline residues have been shown to form an SH3-binding surface in nuclear magnetic resonance analysis and in X-ray crystallography (10, 11, 17), SH3-mediated signaling pathways may not be required for HLA-I down-regulation by Nef. A substitution of only one single amino acid, such as Pro to Ala, may result in a dramatic conformational change. Thus, our results may indicate that Pro78Ala destroyed the Nef structure thoroughly whereas Pro69Ala, Pro72Ala, and Pro75Ala resulted in little conformational change (Fig. 2A and 3A). In other words, Pro78 might be responsible primarily for holding a certain fixed structure and secondarily for down-regulation of HLA-I. However, we prefer the explanation that Pro78 plays a primary role in HLA-I down-regulation, since all the mutant Nefs including PPPA down-regulated CD4 as well as the wild-type. This suggests that their conformational change in mutant Nefs, if any, is minimal.

FlowJo software (Tree Star, San Carlos, Calif.) was used to make configurations. (A) Cells were analyzed for fluorescence intensity in the cell population gated as shown by a circle in each upper panel. The vertical axis represents signal intensity obtained with anti-HLA-I or anti-HLA-C. The horizontal axis represents signal intensity obtained with an anti-CD4 antibody. (B) Histograms of signal intensity obtained with anti-HLA-I or anti-HLA-C. Histograms are overlaid with a dotted-line histogram of an immunoglobulin isotype control. Values are mean fluorescence intensities (MFI) of HLA-I and HLA-C on the cell surface. The data were reproduced in three independent experiments. mock, SeV without inserted genes; Nef, rSeV with wild-type *nef* gene.

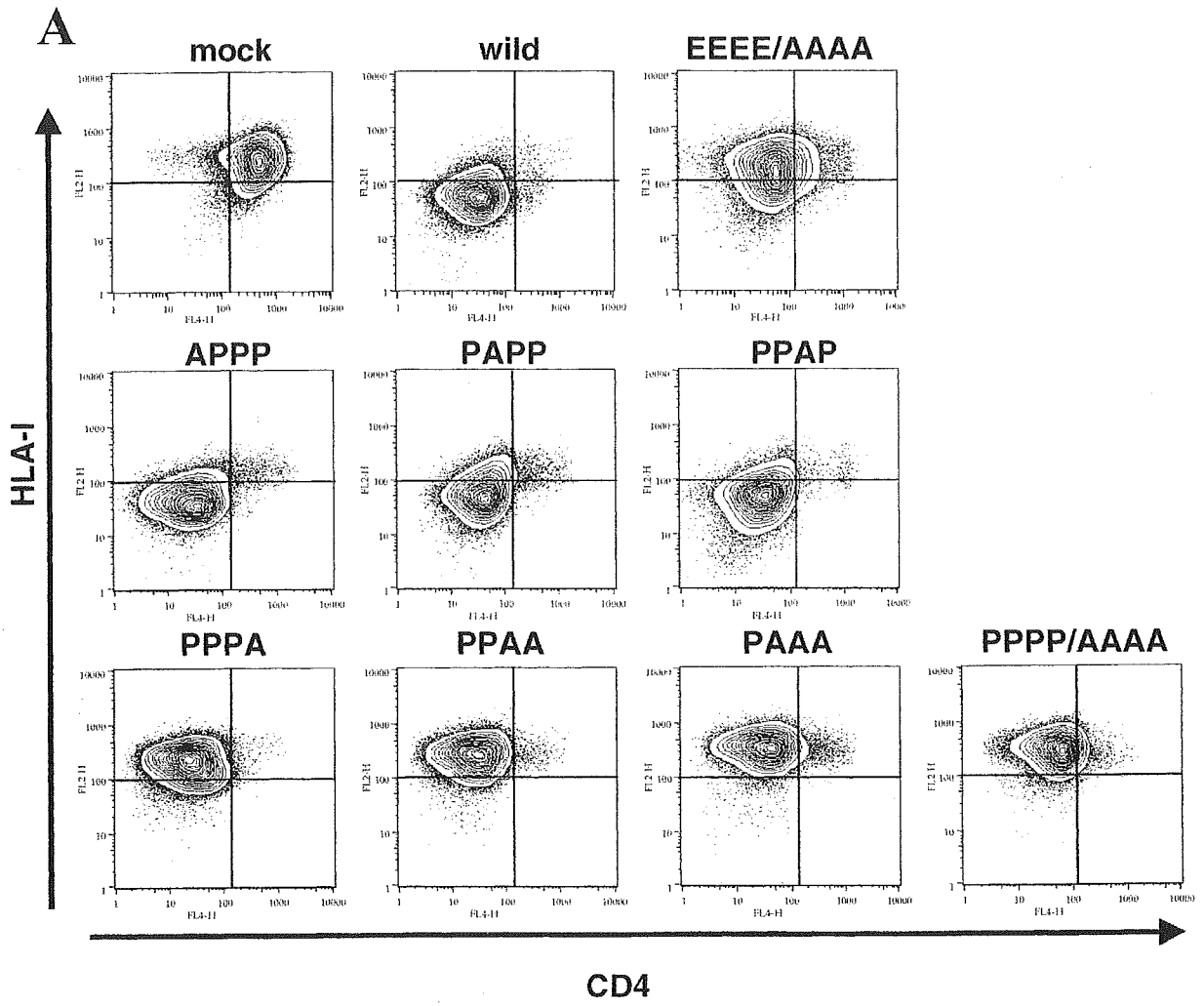


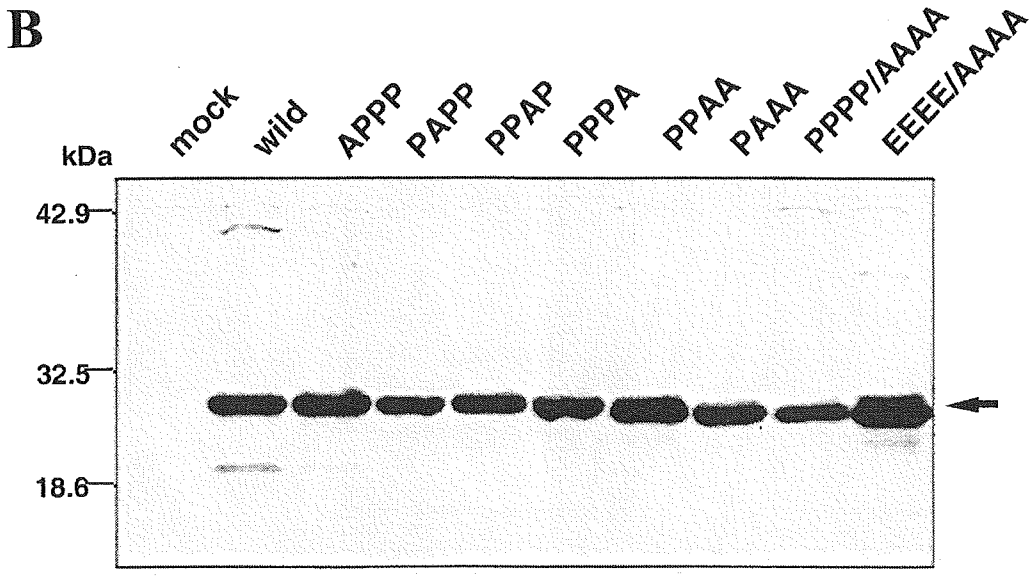


FIG. 2. Analysis of HLA-I down-regulation in CEM cells infected with a series of rSeVs carrying mutant *nef*. CEM cells were infected with each rSeV at a multiplicity of infection of 10 for 1 h. (A) Flow-cytometric analysis of CD4 and HLA-I expression on the cell surface 24 h after infection. The vertical axis represents signal fluorescent intensity obtained with an anti-HLA-I antibody. The horizontal axis represents signal intensity obtained with an anti-CD4 antibody. (B) Cellular expression of Nef proteins by infection with rSeVs. CEM cells ($10^6$) were infected with each rSeV at a multiplicity of infection of 10. One-tenth of the cell lysates was separated by electrophoresis in a sodium dodecyl sulfate–10% polyacrylamide gel. The separated proteins were blotted to a nitrocellulose membrane and stained with an anti-Nef antibody. The arrow indicates bands of about 27 kDa, corresponding to the Nefs shown at the top. The positions of size markers are shown on the left.

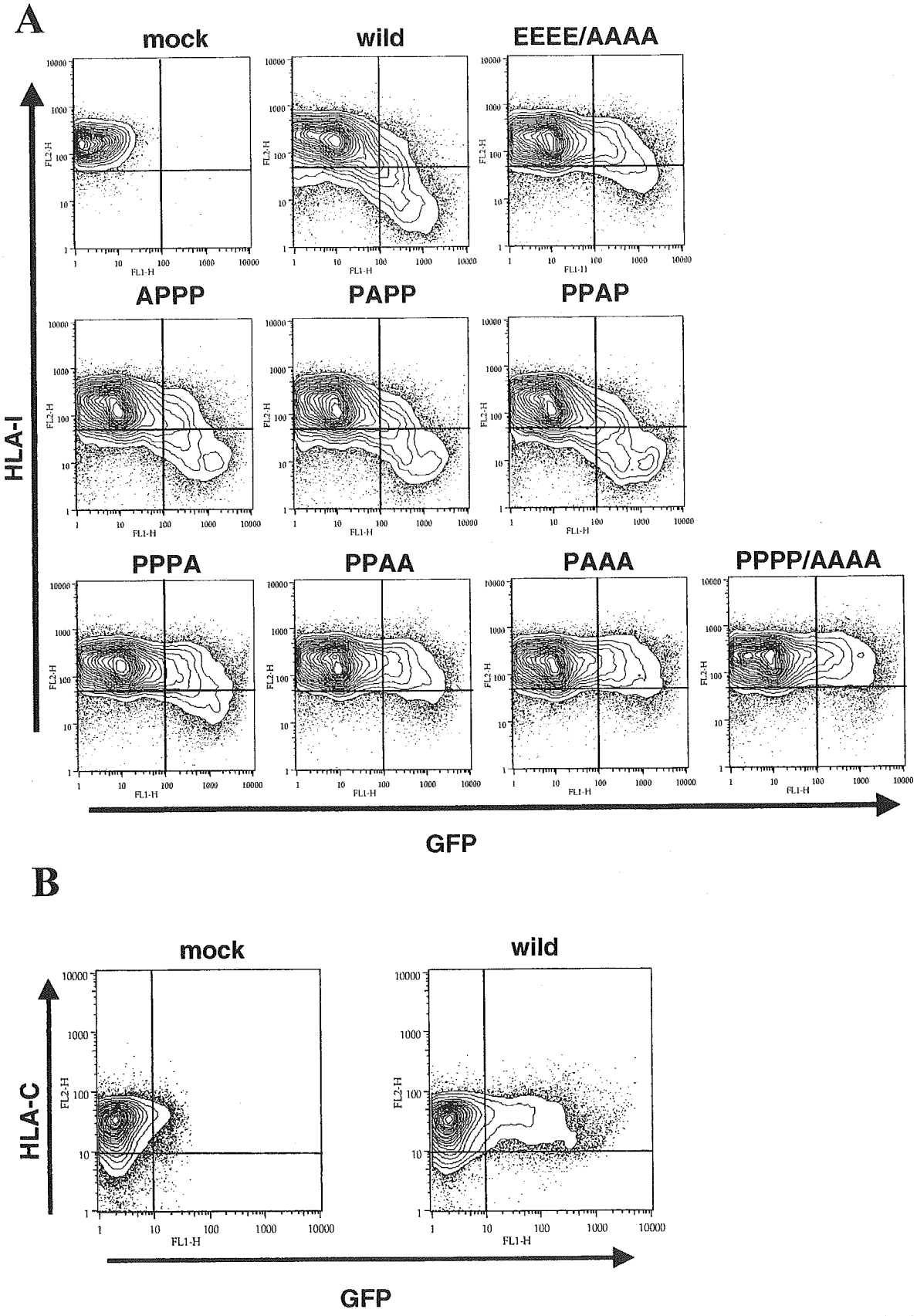


FIG. 3. Flow-cytometric analysis of HIV-1-infected CEM-GFP cells. (A) The vertical axis represents signal intensity obtained with an anti-HLA-I. The horizontal axis represents signal intensity obtained with GFP fluorescence; GFP expression is achieved by HIV-1 infection. The wild-type and mutant Nefs were expressed in the context of HIV-$1_{NL432}$. (B) Surface levels of HLA-C of the cells infected with the wild-type HIV-$1_{NL432}$ were assayed. The vertical axis represents signal intensity obtained with an anti-HLA-C antibody. The horizontal axis represents signal intensity of GFP fluorescence. The results are representative of three independent experiments. mock, non-HIV-1-infected CEM-GFP cells.

We are grateful to Patrizio Giacomini for antibody L31. We thank Mieko Goto and Mariko Tomizawa for technical assistance. We thank Kunito Yoshiike, Tadahito Kanda, and Shinichiro Fuse for critical reading of the manuscript. We thank Akio Nomoto for encouragement.

This work was partly supported by grants for AIDS Research from the Ministry of Health, Labor and Welfare of Japan; a Grant-in-Aid for Scientific Research (A) from Japan Society of the Promotion of Science (JSPS); and the Japan Health Sciences Foundation.

## REFERENCES

1. **Adachi, A., H. E. Gendelman, S. Koenig, T. Folks, R. Willey, A. Rabson, and M. A. Martin.** 1986. Production of acquired immunodeficiency syndrome-associated retrovirus in human and nonhuman cells transfected with an infectious molecular clone. J. Virol. **59:**284–291.
2. **Aiken, C., J. Konner, N. R. Landau, M. E. Lenburg, and D. Trono.** 1994. Nef induces CD4 endocytosis: requirement for a critical dileucine motif in the membrane-proximal CD4 cytoplasmic domain. Cell **76:**853–864.
3. **Cesarman, E., Y. Chang, P. S. Moore, J. W. Said, and D. M. Knowles.** 1995. Kaposi's sarcoma-associated herpesvirus-like DNA sequences in AIDS-related body-cavity-based lymphomas. N. Engl. J. Med. **332:**1186–1191.
4. **Collins, K. L., and D. Baltimore.** 1999. HIV's evasion of the cellular immune response. Immunol. Rev. **168:**65–74.
5. **Collins, K. L., B. K. Chen, S. A. Kalams, B. D. Walker, and D. Baltimore.** 1998. HIV-1 Nef protein protects infected primary cells against killing by cytotoxic T lymphocytes. Nature **391:**397–401.
6. **Craig, H. M., M. W. Pandori, N. L. Riggs, D. D. Richman, and J. C. Guatelli.** 1999. Analysis of the SH3-binding region of HIV-1 nef: partial functional defects introduced by mutations in the polyproline helix and the hydrophobic pocket. Virology **262:**55–63.
7. **Garcia, J. V., and A. D. Miller.** 1991. Serine phosphorylation-independent downregulation of cell-surface CD4 by nef. Nature **350:**508–511.
8. **Gervaix, A., D. West, L. M. Leoni, D. D. Richman, F. Wong-Staal, and J. Corbeil.** 1997. A new reporter cell line to monitor HIV infection and drug susceptibility in vitro. Proc. Natl. Acad. Sci. USA **94:**4653–4658.
9. **Greenberg, M. E., A. J. Iafrate, and J. Skowronski.** 1998. The SH3 domain-binding surface and an acidic motif in HIV-1 Nef regulate trafficking of class I MHC complexes. EMBO J. **17:**2777–2789.
10. **Grzesiek, S., A. Bax, J. S. Hu, J. Kaufman, I. Palmer, S. J. Stahl, N. Tjandra, and P. T. Wingfield.** 1997. Refined solution structure and backbone dynamics of HIV-1 Nef. Protein Sci. **6:**1248–1263.
11. **Grzesiek, S., S. J. Stahl, P. T. Wingfield, and A. Bax.** 1996. The CD4 determinant for downregulation by HIV-1 Nef directly binds to Nef. Mapping of the Nef binding surface by NMR. Biochemistry **35:**10256–10261.
12. **Hasan, M. K., A. Kato, T. Shioda, Y. Sakai, D. Yu, and Y. Nagai.** 1997. Creation of an infectious recombinant Sendai virus expressing the firefly luciferase gene from the 3′ proximal first locus. J. Gen. Virol. **78:**2813–2820.
13. **Hengel, H., and U. H. Koszinowski.** 1997. Interference with antigen processing by viruses. Curr. Opin. Immunol. **9:**470–476.
14. **Ho, S. N., H. D. Hunt, R. M. Horton, J. K. Pullen, and L. R. Pease.** 1989. Site-directed mutagenesis by overlap extension using the polymerase chain reaction. Gene **77:**51–59.
15. **Ishido, S., C. Wang, B. S. Lee, G. B. Cohen, and J. U. Jung.** 2000. Downregulation of major histocompatibility complex class I molecules by Kaposi's sarcoma-associated herpesvirus K3 and K5 proteins. J. Virol. **74:**5300–5309.
16. **Janvier, K., C. Petit, E. Le Rouzic, O. Schwartz, and S. Benichou.** 2000. HIV auxiliary proteins: an interface between the virus and the host. AIDS **14:** S21–S30.
17. **Lee, C. H., K. Saksela, U. A. Mirza, B. T. Chait, and J. Kuriyan.** 1996. Crystal structure of the conserved core of HIV-1 Nef complexed with a Src family SH3 domain. Cell **85:**931–942.
18. **Le Gall, S., F. Buseyne, A. Trocha, B. D. Walker, J. M. Heard, and O. Schwartz.** 2000. Distinct trafficking pathways mediate Nef-induced and clathrin-dependent major histocompatibility complex class I down-regulation. J. Virol. **74:**9256–9266.
19. **Lim, W. A.** 1996. Reading between the lines: SH3 recognition of an intact protein. Structure **4:**657–659.
20. **Mangasarian, A., V. Piguet, J. K. Wang, Y. L. Chen, and D. Trono.** 1999. Nef-induced CD4 and major histocompatibility complex class I (MHC-I) down-regulation are governed by distinct determinants: N-terminal alpha helix and proline repeat of Nef selectively regulate MHC-I trafficking. J. Virol. **73:**1964–1973.
21. **Nagai, Y., and A. Kato.** 1999. Paramyxovirus reverse genetics is coming of age. Microbiol. Immunol. **43:**613–624.
22. **Nicholas, J., V. Ruvolo, J. Zong, D. Ciufo, H. G. Guo, M. S. Reitz, and G. S. Hayward.** 1997. A single 13-kilobase divergent locus in the Kaposi sarcoma-associated herpesvirus (human herpesvirus 8) genome contains nine open reading frames that are homologous to or related to cellular proteins. J. Virol. **71:**1963–1974.
23. **Piguet, V., L. Wan, C. Borel, A. Mangasarian, N. Demaurex, G. Thomas, and D. Trono.** 2000. HIV-1 Nef protein binds to the cellular protein PACS-1 to downregulate class I major histocompatibility complexes. Nat. Cell Biol. **2:**163–167.
24. **Ploegh, H. L.** 1998. Viral strategies of immune evasion. Science **280:**248–253.
25. **Riggs, N. L., H. M. Craig, M. W. Pandori, and J. C. Guatelli.** 1999. The dileucine-based sorting motif in HIV-1 Nef is not required for down-regulation of class I MHC. Virology **258:**203–207.
26. **Russo, J. J., R. A. Bohenzky, M. C. Chien, J. Chen, M. Yan, D. Maddalena, J. P. Parry, D. Peruzzi, I. S. Edelman, Y. Chang, and P. S. Moore.** 1996. Nucleotide sequence of the Kaposi sarcoma-associated herpesvirus (HHV8). Proc. Natl. Acad. Sci. USA **93:**14862–14867.
27. **Sakai, Y., K. Kiyotani, M. Fukumura, M. Asakawa, A. Kato, T. Shioda, T. Yoshida, A. Tanaka, M. Hasegawa, and Y. Nagai.** 1999. Accommodation of foreign genes into the Sendai virus genome: sizes of inserted genes and viral replication. FEBS Lett. **456:**221–226.
28. **Schwartz, O., V. Marechal, S. Le Gall, F. Lemonnier, and J. M. Heard.** 1996. Endocytosis of major histocompatibility complex class I molecules is induced by the HIV-1 Nef protein. Nat. Med. **2:**338–342.
29. **Setini, A., A. Beretta, C. De Santis, R. Meneveri, A. Martayan, M. C. Mazzilli, E. Appella, A. G. Siccardi, P. G. Natali, and P. Giacomini.** 1996. Distinctive features of the alpha 1-domain alpha helix of HLA-C heavy chains free of beta 2-microglobulin. Hum. Immunol. **46:**69–81.
30. **Toriyoshi, H., T. Shioda, H. Sato, M. Sakaguchi, Y. Eda, S. Tokiyoshi, K. Kato, K. Nohtomi, S. Kusagawa, K. Taniguchi, T. Shiino, A. Kato, S. Foongladda, S. Linkanonsakul, S. I. Oka, A. Iwamoto, C. Wasi, Y. Nagai, and Y. Takebe.** 1999. Sendai virus-based production of HIV type 1 subtype B and subtype E envelope glycoprotein 120 antigens and their use for highly sensitive detection of subtype-specific serum antibodies. AIDS Res. Hum. Retrovir. **15:**1109–1120.
31. **Yu, D., T. Shioda, A. Kato, M. K. Hasan, Y. Sakai, and Y. Nagai.** 1997. Sendai virus-based expression of HIV-1 gp120: reinforcement by the V(−) version. Genes Cells **2:**457–466.

*Journal of Thrombosis and Haemostasis*, **2**: 754–762

ORIGINAL ARTICLE

# Induction of immune tolerance by neonatal intravenous injection of human factor VIII in murine hemophilia A

S. MADOIWA, T. YAMAUCHI,† Y. HAKAMATA,* E. KOBAYASHI,* M. ARAI,‡ T. SUGO, J. MIMURO and Y. SAKATA

*Divisions of Cell and Molecular Medicine and *Organ Replacement Research, Center for Molecular Medicine, and †Department of Pediatrics, Jichi Medical School, Minamikawachi-machi, Tochigi, Japan; and ‡Department of Laboratory Medicine, Tokyo Medical University, Shinjuku-ku, Japan*

**To cite this article:** Madoiwa S, Yamauchi T, Hakamata Y, Kobayashi E, Arai M, Sugo T, Mimuro J, Sakata Y. Induction of immune tolerance by neonatal intravenous injection of human factor VIII in murine hemophilia A. *J Thromb Haemost* 2004; **2**: 754–62.

**Summary.** Inhibitory antibody formation is the most serious complication of factor (F)VIII replacement therapy in hemophilia A patients. FVIII-deficient mice were used to study new approaches for induction of immune tolerance. Neither anti-FVIII inhibitory antibodies nor antiFVIII IgGs were observed in 13 of 14 adult mice that received 0.05 U $g^{-1}$ body weight of human FVIII intravenously within 24 h after birth and repeated injections as adults. In contrast, high FVIII antibody titers (> 50 Bethesda Units $mL^{-1}$) developed in seven of 13 mice injected on day 3 postpartum and in all adult mice not treated neonatally. One of nine mice and three of 17 mice developed high-titer antiFVIII inhibitory antibody when they were treated initially with 2-fold (0.1 U $g^{-1}$ body weight) and 10-fold higher doses (0.5 U $g^{-1}$ body weight) FVIII on day 0, respectively. A human FVIII-specific T-cell proliferative response was absent in splenocytes from neonatally treated mice. The tolerance was FVIII specific because antitoxoid antibodies developed after immunization with tetanus toxoid. Splenocytes failed to proliferate or produce interferon (IFN)-γ in response to FVIII stimulation, yet still secreted interleukin-2. A proliferative response was restored with exogenous IFN-γ or interleukin-12, suggesting that lack of inhibitor to FVIII was due to IFN-γ-dependent anergy. Thus, exposure on day 0 to physiological levels of FVIII antigen might be important for induction of immune tolerance. This immune tolerance model may provide a basis for new approaches to prevention of FVIII inhibitors during replacement therapy.

**Keywords**: factor VIII-deficient mice, hemophilia A, immune tolerance, neonate.

Correspondence: Yoichi Sakata, Division of Cell and Molecular Medicine, Center for Molecular Medicine, Jichi Medical School, Minamikawachi-machi, Tochigi 329-0498, Japan.
Tel.: +81 285 58 7398; fax: +81 285 44 7817; e-mail: yoisaka@jichi.ac.jp

Received 10 June 2003, accepted 18 December 2003

## Introduction

Hemophilia A is an X-linked, recessive hereditary bleeding disorder due to deficient coagulation factor (F)VIII [1]. Patients with severe hemophilia A require frequent infusions of plasma-derived or recombinant FVIII to correct their clotting deficiency. However, approximately 30% of patients develop inhibitors or circulating alloantibodies against FVIII following replacement therapy [2]. Once an inhibitor develops, treatment of bleeding episodes is quite difficult due to rapid inactivation of infused FVIII. The current strategy to eradicate inhibitors is immune tolerance induction with frequent infusions of high FVIII doses [3,4], even though this therapy is very expensive [5,6].

During the neonatal period, the developing immune system is particularly susceptible to induction of tolerance [7–12]. Since normal adult mice are partially tolerant to human FVIII [13], they are not considered to be a suitable model for study of immune tolerance induction in neonates. Hemophilia A mice are generated by targeted disruption of exons 16 or 17 of the FVIII gene, and are suitable models for human severe hemophilia A [14]. They have < 1% of the FVIII activity of normal mice, absence of FVIII light chain protein, impaired hemostasis, severe bleeding after minor injuries, and spontaneous bleeding [15]. The mice typically develop an antiFVIII immune response against experimental treatment, such as multiple intravenous injections of human FVIII [16–19]. Although precise injection into the tiny blood vessels of neonates requires some expertise, it is essential to evaluate the effect of neonatal exposure of antigen on newborn immunity.

In this study, we demonstrate that neonatal intravenous administration of physiological human FVIII doses induces long-term tolerance in hemophilia A mice, giving rise to possible new approaches to treatment of hemophilia A patients.

## Materials and methods

### *Hemophilic mice*

Hemophilic mice with targeted destruction of exon 16 of the FVIII gene were kindly provided by H. H. Kazazian Jr